

1  
2  
3 **Granger causality from the first and second**  
4 **differences of atmospheric CO<sub>2</sub> to global**  
5 **surface temperature and the El Niño–Southern**  
6 **Oscillation respectively**

7  
8 **L.M.W. Leggett <sup>1</sup> and D.A. Ball <sup>1</sup>**

9 (1) (Global Risk Policy Group Pty Ltd, Townsville, Queensland, Australia)

10 [www.globalriskprogress.com](http://www.globalriskprogress.com)

11 Correspondence to: L.M.W. Leggett ([mleggett.globalriskprogress@gmail.com](mailto:mleggett.globalriskprogress@gmail.com))

12  
13  
14 **Abstract**

15  
16 A significant gap now of some 16 years in length has been shown to exist between the  
17 observed global surface temperature trend and that expected from the majority of  
18 climate simulations, and this gap is presently continuing to increase. For its own sake,  
19 and to enable better climate prediction for policy use, the reasons behind this  
20 mismatch need to be better understood. While an increasing number of possible  
21 causes have been proposed, the candidate causes have not yet converged.

22  
23 The standard model which is now displaying the disparity has it that temperature will  
24 rise roughly linearly with atmospheric CO<sub>2</sub>. However research also exists showing  
25 correlation between the interannual variability in the growth rate of atmospheric CO<sub>2</sub>  
26 and temperature. Rate of change of CO<sub>2</sub> had not been considered a causative  
27 mechanism for temperature because it was concluded that causality ran from  
28 temperature to rate of change of CO<sub>2</sub>.

29  
30 However more recent studies have found little or no evidence for temperature leading  
31 rate of change of CO<sub>2</sub> but instead evidence for simultaneity. With this background,  
32 this paper reinvestigates the relationship between rate of change of CO<sub>2</sub> and two of the

1 major climate variables, atmospheric temperature and the El Niño–Southern  
2 Oscillation (ENSO).

3  
4 Using time series analysis in the form of dynamic regression modelling with  
5 autocorrelation correction, it is demonstrated that first-difference CO<sub>2</sub> leads  
6 temperature and that there is a highly statistically significant correlation between first-  
7 difference CO<sub>2</sub> and temperature. Further, a correlation is found for second-difference  
8 CO<sub>2</sub> with the Southern Oscillation Index, the atmospheric-pressure component of  
9 ENSO. This paper also demonstrates that both these correlations display Granger  
10 causality.

11  
12 It is shown that the first-difference CO<sub>2</sub> and temperature model shows no trend  
13 mismatch in recent years.

14  
15 These results may contribute to the prediction of future trends for global temperature  
16 and ENSO.

17  
18 Interannual variability in the growth rate of atmospheric CO<sub>2</sub> is standardly attributed  
19 to variability in the carbon sink capacity of the terrestrial biosphere. The terrestrial  
20 biosphere carbon sink is created by the difference between photosynthesis and  
21 respiration (net primary productivity): a major way of measuring global terrestrial  
22 photosynthesis is by means of satellite measurements of vegetation reflectance, such  
23 as the Normalized Difference Vegetation Index (NDVI). In a preliminary analysis,  
24 this study finds a close correlation between an increasing NDVI and the increasing  
25 climate model/temperature mismatch (as quantified by the difference between the  
26 trend in the level of CO<sub>2</sub> and the trend in temperature).

27

28

29

30

## 31 **1 Introduction**

32

33 Understanding current global climate requires an understanding of trends both in  
34 Earth's atmospheric temperature and the El Niño–Southern Oscillation (ENSO), a

1 characteristic large-scale distribution of warm water in the tropical Pacific Ocean and  
2 the dominant global mode of year-to-year climate variability (Holbrook et al. 2009).  
3 However, despite much effort, the average projection of current climate models has  
4 become statistically significantly different from the 21st century global surface  
5 temperature trend (Fyfe et al. 2013; Fyfe and Gillett 2014) and has failed to reflect the  
6 statistically significant evidence that annual-mean global temperature has not risen in  
7 the 21st century (Fyfe et al. 2013; Kosaka and Shang-Ping 2013).

8

9 The situation is illustrated visually in Figure 1 which shows the increasing departure  
10 over recent years of the global surface temperature trend from that projected by a  
11 representative mid-range global climate model (GCM) for global surface temperature  
12 - the CMIP3, SRESA1B scenario model (Meehl et al. 2007). It is noted that the level  
13 of atmospheric CO<sub>2</sub> is a good proxy for the International Panel on Climate Change  
14 (IPCC) models predicting the global surface temperature trend: according to IPCC  
15 (2014), on decadal to interdecadal time scales and under continually increasing  
16 effective radiative forcing, the forced component of the global surface temperature  
17 trend responds to the forcing trend relatively rapidly and almost linearly.

18

19 Modelling also provides a wide range of predictions for future ENSO variability,  
20 some showing an increase, others a decrease, and some no change (Guilyardi et al.  
21 2012; Bellenger 2013). The extremes of this ENSO variability cause extreme weather  
22 events (such as floods and droughts) in many regions of the world.

23 A wide range of physical explanations has now been proposed for the global warming  
24 slowdown. These involve proposals either for changes in the way the radiative  
25 mechanism itself is working or for the increased influence of other physical  
26 mechanisms. Chen and Tung (2014) place these proposed explanations into two  
27 categories. The first involves a reduction in radiative forcing: by a decrease in  
28 stratospheric water vapour, an increase in background stratospheric volcanic aerosols,  
29 by 17 small volcano eruptions since 1999, increasing coal-burning in China, the  
30 indirect effect of time-varying anthropogenic aerosols, a low solar minimum, or a  
31 combination of these. The second category of candidate explanation involves  
32 planetary sinks for the excess heat. The major focus for the source of this sink has  
33 been physical and has involved ocean heat sequestration. However, evidence for the  
34 precise nature of the ocean sinks is not yet converging: according to Chen and Tung

1 (2014) their study followed the original proposal of Meehl et al. (2011) that global  
2 deep-ocean heat sequestration is centred on the Pacific. However, their observational  
3 results were that such deep-ocean heat sequestration is mainly occurring in the  
4 Atlantic and the Southern oceans.

5  
6 Alongside the foregoing possible physical causes, Hansen et al. (2013) have suggested  
7 that the mechanism for the pause in the global temperature increase since 1998 might  
8 be the planetary biota, in particular the terrestrial biosphere: that is (IPCC 2007), the  
9 fabric of soils, vegetation and other biological components, the processes that connect  
10 them and the carbon, water and energy that they store.

11  
12 It is widely considered that the interannual variability in the growth rate of  
13 atmospheric CO<sub>2</sub> is a sign of the operation of the influence of the planetary biota.

14 Again, IPCC (2007) states: “The atmospheric CO<sub>2</sub> growth rate exhibits large  
15 interannual variations. The change in fossil fuel emissions and the estimated  
16 variability in net CO<sub>2</sub> uptake of the oceans are too small to account for this signal,  
17 which must be caused by year-to-year fluctuations in land-atmosphere fluxes.”

18 In the IPCC Fourth Assessment Report, Denman et al. (2007) state (italics denote  
19 present author emphasis): “Interannual and inter-decadal variability in the growth rate  
20 of atmospheric CO<sub>2</sub> is dominated by the *response of the land biosphere to climate*  
21 *variations*. .... The terrestrial biosphere *interacts strongly with the climate*, providing  
22 both positive and negative feedbacks due to biogeophysical and biogeochemical  
23 processes. ... Surface climate is determined by the balance of fluxes, which can be  
24 changed by radiative (e.g., albedo) or non-radiative (e.g., water cycle related  
25 processes) terms. Both radiative and non-radiative terms *are controlled by details of*  
26 *vegetation*.”

27  
28 Denman et al. (2007) also note that many studies have confirmed that the variability  
29 of CO<sub>2</sub> fluxes is mostly due to land fluxes, and that tropical lands contribute strongly  
30 to this signal. A predominantly terrestrial origin of the growth rate variability can be  
31 inferred from (1) atmospheric inversions assimilating time series of CO<sub>2</sub>  
32 concentrations from different stations, (2) consistent relationships between δ<sup>13</sup>C and  
33 CO<sub>2</sub>, (3) ocean model simulations, and (4) terrestrial carbon cycle and coupled model  
34 simulations. For one prominent estimate carried out by the Global Carbon Project, the

1 land sink is calculated as the residual of the sum of all sources minus the sum of the  
2 atmosphere and ocean sinks (Le Quere et al. 2014).

3  
4 The activity of the land sink can also be estimated directly. The terrestrial biosphere  
5 carbon sink is created by photosynthesis: a major way of measuring global land  
6 photosynthesis is by means of satellite measurements of potential photosynthesis from  
7 greenness estimates. The measure predominantly used is the Normalized Difference  
8 Vegetation Index (NDVI) (Running et al. 2004; Zhang et al. 2014). NDVI data are  
9 available from the start of satellite observations in 1980 to the present. For this period  
10 the trend signature in NDVI has been shown to correlate closely with that for  
11 atmospheric CO<sub>2</sub> (Barichivich et al. 2013). This noted, we have not been able to find  
12 studies which have compared NDVI data with the difference between climate models  
13 and temperature.

## 14 15 16 **2 Methodological issues and objectives of the study**

### 17 **2.1 Methodological issues**

18  
19 Before considering further material it is helpful now to consider a range of  
20 methodological issues and concepts. The first concept is to do with the notion of  
21 causality.

22  
23 According to Hidalgo and Sekhon (2011) there are four prerequisites to enable an  
24 assertion of causality. The first is that the cause must be prior to the effect. The  
25 second prerequisite is “constant conjunction” between variables (Hume (1751), cited  
26 in Hidalgo and Sekhon (2011)). This relates to the degree of fit between variables.  
27 The final requirements are those concerning manipulation and random placement into  
28 experimental and control categories. It is noted that each of the four prerequisites is  
29 necessary but not sufficient on its own for causality.

30  
31 With regard to the last two criteria, the problem for global studies such as global  
32 climate studies is that manipulation and random placement into experimental and  
33 control categories cannot be carried out.

1 One method using correlational data, however, approaches more closely the quality of  
2 information derived from random placement into experimental and control categories.  
3 The concept is that of Granger causality (Granger 1969). According to Stern and  
4 Kaufmann (2014), a time series variable “ $x$ ” (e.g. atmospheric CO<sub>2</sub>) is said to  
5 “Granger-cause” variable “ $y$ ” (e.g. surface temperature) if past values of  $x$  help predict  
6 the current level of  $y$ , better than do just the past values of  $y$ , given all other relevant  
7 information.

8  
9 Reference to the above four aspects of causality will be made to help structure the  
10 review of materials in the following sections.

11  
12

### 13 **2.2 Objectives of the study**

14

15 What has been considered to influence the biota’s creation of the pattern observed in  
16 the trend in the growth rate of atmospheric CO<sub>2</sub>? The candidates for the influences on  
17 the biota have mainly been considered in prior research to be atmospheric variations,  
18 primarily temperature and/or ENSO (e.g., Kuo et al. 1990; Wang W. et al. 2013).

19 Despite its proposed role in global warming overall, CO<sub>2</sub> (in terms of the initial state  
20 of atmospheric CO<sub>2</sub> exploited by plants at time  $A$ ) has not generally been isolated and  
21 studied in detail through time series analysis as an influence in the way the biosphere  
22 influences the CO<sub>2</sub> left in the atmosphere at succeeding time  $B$ .

23

24 This lack of attention to the influence of the biosphere on climate variables seems to  
25 have come about for two reasons, one concerning ENSO, the other, temperature. For  
26 ENSO, the reason is that the statistical studies are unambiguous that ENSO leads rate  
27 of change of CO<sub>2</sub> (e.g., Lean and Rind 2008). On the face of it, therefore, this ruled  
28 out CO<sub>2</sub> as the first mover of the ecosystem processes. For temperature, the reason  
29 was that the question of whether atmospheric temperature leads rate of change of CO<sub>2</sub>  
30 or vice versa is less settled.

1 In the first published study on this question, Kuo et al. (1990) provided evidence that  
2 the signature of interannual atmospheric CO<sub>2</sub> (measured as its first-difference) fitted  
3 temperature (passing therefore one of the four tests for causality, of close conjunction).

4 The relative fits of both level of and first-difference of atmospheric CO<sub>2</sub> with global  
5 surface temperature up to the present are depicted in Figure 2. Attention is drawn to  
6 both signature (fine grained data structure) and, by means of polynomial smoothing,  
7 core trend for each data series.

8 Concerning signature, while clearly first-difference CO<sub>2</sub> and temperature are not  
9 identical, each is more alike than either is to the temperature model based on level of  
10 CO<sub>2</sub>. As well, the polynomial fits show that the same likeness groupings exist for core  
11 trend.

12 Kuo et al. (1990) also provided evidence concerning another of the causality  
13 prerequisites – priority. This was that the signature of first-difference CO<sub>2</sub> *lagged*  
14 temperature (by 5 months). This idea has been influential. More recently, Adams and  
15 Piovesan (2005) noted that climate variations acting on ecosystems are believed to be  
16 responsible for variation in CO<sub>2</sub> increment, but there are major uncertainties in  
17 identifying processes, including uncertainty concerning *instantaneous* (present  
18 authors' emphasis) versus lagged responses. Wang et al. (2013) observed that the  
19 strongest coupling is found between the CO<sub>2</sub> growth rate and the *concurrent* (present  
20 authors' emphasis) tropical land temperature. Wang et al. (2013) nonetheless state in  
21 their conclusion that the strong temperature–CO<sub>2</sub> coupling they observed is best  
22 explained by the additive responses of tropical terrestrial respiration and primary  
23 production to temperature variations, which reinforce each other in enhancing  
24 *temperature's control* (present author emphasis) on tropical net ecosystem exchange.

25 Another perspective on the relative effects of rising atmospheric CO<sub>2</sub> concentrations  
26 on the one hand and temperature on the other has been provided by extensive direct  
27 experimentation on plants. In a large scale meta-analysis of such experiments,  
28 Dieleman et al. (2012) drew together results on how ecosystem productivity and soil  
29 processes responded to combined warming and CO<sub>2</sub> manipulation, and compared it  
30 with those obtained from single factor CO<sub>2</sub> and temperature manipulation. While the  
31 meta-analysis found that responses to combined CO<sub>2</sub> and temperature treatment

1 showed the greatest effect, this was only slightly larger than for the CO<sub>2</sub>-only  
2 treatment. By contrast, the effect of the CO<sub>2</sub>-only treatment was markedly larger than  
3 for the warming-only treatment.

4  
5 In looking at leading and lagging climate series more generally, the first finding of  
6 correlations between the rate of change (in the form of the first-difference) of  
7 atmospheric CO<sub>2</sub> and a climate variable was with the foregoing and the Southern  
8 Oscillation Index (SOI) component of ENSO (Bacastow 1976). Here evidence was  
9 presented that the SOI led first-difference atmospheric CO<sub>2</sub>. There have been further  
10 such studies (see Imbers (2013) for overview) which, taken together, consistently  
11 show that the highest correlations are achieved with SOI leading temperature by some  
12 months (3-4 months).

13  
14 In light of the foregoing, this paper reanalyses by means of time series regression  
15 analysis which of first-difference CO<sub>2</sub> and temperature lead. The joint temporal  
16 relationship between interannual atmospheric CO<sub>2</sub>, global surface temperature and  
17 ENSO (indicated by the SOI) is also investigated.

18  
19 The foregoing also shows that a strong case can be made for further investigating the  
20 planetary biota influenced by atmospheric CO<sub>2</sub> as a candidate influence on (cause of)  
21 climate outcomes. This question is also explored in this paper.

22  
23 A number of Granger causality studies have been carried out on climate time series  
24 (see review in Attanasio 2012). We found six papers which assessed atmospheric CO<sub>2</sub>  
25 and global surface temperature (Sun and Wang 1996; Triacca 2005; Kodra et al. 2011;  
26 Attanasio and Triacca 2011; Attanasio 2012; Stern and Kaufmann 2014). Of these,  
27 while all but one (Triacca 2005) found Granger causality, it was not with CO<sub>2</sub>  
28 concentration as studied in this paper but with CO<sub>2</sub> radiative forcing (lnCO<sub>2</sub>  
29 (Attanasio and Triacca 2011)).

30  
31 As well, all studies used annual not monthly data. Such annual data for each of  
32 atmospheric CO<sub>2</sub> and temperature is not stationary of itself but must be transformed  
33 into a new, stationary, series by differencing (Sun and Wang 1996). Further, data at

1 this level of aggregation can "mask" correlational effects that only become apparent  
2 when higher frequency (e.g., monthly) data are used.

3  
4 Rather than using a formal Granger causality analysis, a number of authors have  
5 instead used conventional multiple regression models in attempts to quantify the  
6 relative importance of natural and anthropogenic influencing factors on climate  
7 outcomes such as global surface temperature. These regression models use  
8 contemporaneous explanatory variables. For example, see Lean and Rind (2008,  
9 2009); Foster and Rahmstorf (2011); Kopp and Lean (2011); Zhou and Tung (2013).  
10 This type of analysis effectively assumes a causal direction between the variables  
11 being modelled. It is incapable of providing a proper basis for testing for the presence  
12 or absence of causality. In some cases account has been taken of autocorrelation in the  
13 model's errors, but this does not overcome the fundamental weakness of standard  
14 multiple regression in this context. In contrast, Granger causality analysis that we  
15 adopt in this paper provides a formal testing of both the presence and direction  
16 of this causality (Granger 1969).

17  
18 From such studies, a common set of main influencing factors (also called explanatory  
19 or predictor variables) has emerged. These are (Lockwood (2008); Folland (2013);  
20 Zhou and Tung (2013)): El Nino–Southern Oscillation (ENSO), or Southern  
21 Oscillation Index (SOI) alone; volcano aerosol optical depth; total solar irradiance;  
22 and the trend in anthropogenic greenhouse gas (the predominant anthropogenic  
23 greenhouse gas being CO<sub>2</sub>). In these models, ENSO/SOI is the factor embodying  
24 interannual variation. Imbers et al. (2013) show that a range of different studies using  
25 these variables have all produced similar and close fits with the global surface  
26 temperature.

27  
28 With this background, this paper first presents an analysis concerning whether the  
29 first-difference of atmospheric CO<sub>2</sub> leads or lags global surface temperature. After  
30 assessing this, questions of autocorrelation, strength of correlation, and of causality  
31 are then explored. Given this exploration of correlations involving first-difference  
32 atmospheric CO<sub>2</sub>, the possibility of the correlation of second-difference CO<sub>2</sub> with  
33 climate variables is also explored.

34

1  
2 Correlations are assessed at a range of time scales to seek the time extent over which  
3 relationships are held, and thus whether they are a special case or possibly longer term  
4 in nature. The time scales involved are, using instrumental data, over two periods  
5 starting respectively from 1959 and 1877; and, using paleoclimate data, over a period  
6 commencing from 1515. The correlations are assessed by means of regression models  
7 explicitly incorporating autocorrelation using dynamic modelling methods. Granger  
8 causality between CO<sub>2</sub> and, respectively, temperature and SOI is also explored.  
9 Atmospheric CO<sub>2</sub> rather than emissions data is used, and where possible at monthly  
10 rather than annual aggregation. Finally, as noted, we have not been able to find studies  
11 which have compared the gap between climate models and temperature with NDVI  
12 data, so an assessment of this question is carried out. All assessments were carried out  
13 using the time series statistical software packages Gnu Regression, Econometrics and  
14 Time-series Library (GRETTL) (Available from: <http://gretl.sourceforge.net/> (Accessed  
15 January 23, 2014)) and IHS Eviews (IHS EViews 2011).

16  
17  
18

### 19 **3. Data and methods**

20  
21

22 We present results of time series analyses of climate data. The data assessed are  
23 global surface temperature, atmospheric carbon dioxide (CO<sub>2</sub>) and the Southern  
24 Oscillation Index (SOI). The regressions are presented in several batches based on the  
25 length of data series for which the highest temporal resolution is available. The first  
26 batch of studies involves the data series for which the available high resolution series  
27 is shortest: this is for atmospheric carbon dioxide (CO<sub>2</sub>) and commences in 1958.

28 These studies are set at monthly resolution.

29

30 The second batch of studies is for data able to be set at monthly resolution not  
31 involving CO<sub>2</sub>. These studies begin with the time point at which the earliest available  
32 monthly SOI data commences, 1877.

33

34 The final batch of analyses utilises annual data. These studies use data starting  
35 variously in the 16<sup>th</sup> or 18<sup>th</sup> centuries.

1  
2  
3  
4  
5  
6  
7  
8  
9  
10  
11  
12  
13  
14  
15  
16  
17  
18  
19  
20  
21  
22  
23  
24  
25  
26  
27  
28  
29  
30  
31  
32  
33  
34

Data from 1877 and more recently are from instrumental sources; earlier data are from paleoclimate sources.

For instrumental data sources for global surface temperature, we used the Hadley Centre–Climate Research Unit combined land SAT and SST (HadCRUT) version 4.2.0.0 (Morice et al. 2012), for atmospheric CO<sub>2</sub>, the U.S. Department of Commerce National Oceanic & Atmospheric Administration Earth System Research Laboratory Global Monitoring Division Mauna Loa, Hawaii, monthly CO<sub>2</sub> series (Keeling et al. 2009), and for volcanic aerosols the National Aeronautic and Space Administration Goddard Institute for Space Studies Stratospheric Aerosol Optical Thickness series (Sato et al. 1993). Southern Oscillation Index data (Troup 1965) is from the Science Delivery Division of the Department of Science, Information Technology, Innovation and the Arts (DSITIA) Queensland, Australia. Solar irradiance data is from Lean, J. (personal communication 2012).

With regard to the El Niño-Southern Oscillation, according to IPCC (2014) the term El Niño was initially used to describe a warm-water current that periodically flows along the coast of Ecuador and Peru, disrupting the local fishery. It has since become identified with a basin-wide warming of the tropical Pacific Ocean east of the dateline. This oceanic event is associated with a fluctuation of a global-scale tropical and subtropical surface atmospheric pressure pattern called the Southern Oscillation. This atmosphere–ocean phenomenon is coupled, with typical time scales of two to about seven years, and known as the El Niño-Southern Oscillation (ENSO).

The El Niño (temperature) component of ENSO is measured by changes in the sea surface temperature of the central and eastern equatorial Pacific relative to the average temperature. The Southern Oscillation (atmospheric pressure) ENSO component is often measured by the surface pressure anomaly difference between Tahiti and Darwin.

For the present study we choose the SOI atmospheric pressure component rather than the temperature component of ENSO to stand for ENSO as a whole. This is because it is considered to be more valid to conduct an analysis in which temperature is an

1 outcome (dependent variable) without also having temperature as an input  
2 (independent variable). The correlation between SOI and the other ENSO indices is  
3 high, so we believe this assumption is robust.

4  
5  
6

7 Paleoclimate data sources are: Atmospheric CO<sub>2</sub>, from 1500 – ice cores (Robertson et  
8 al. (2001)); (NH) temperature, from 1527 – tree ring data (Moberg, A. et al. 2005;  
9 SOI, from 1706 – tree ring data (Stahle et al. (1998)).

10

11 Normalized Difference Vegetation Index (NDVI) monthly data from 1980 to 2006 is  
12 from the GIMMS (Global Inventory Modeling and Mapping Studies) data set (Tucker  
13 et al. 2005) . NDVI data from 2006 to 2013 was provided by the Institute of  
14 Surveying, Remote Sensing and Land Information, University of Natural Resources  
15 and Life Sciences, Vienna.

16

17 Statistical methods used are standard (Greene 2012). Categories of methods used are:  
18 normalisation; differentiation (approximated by differencing); and time series analysis.  
19 Within time series analysis, methods used are: smoothing; leading or lagging of data  
20 series relative to one another to achieve best fit; assessing a prerequisite for using data  
21 series in time series analysis, that of stationarity; including autocorrelation in models  
22 by use of dynamic regression models; and investigating causality by means of a  
23 multivariate time series model, known as a vector autoregression (VAR) and its  
24 associated Granger causality test. These methods will now be described in turn.

25

26 To make it easier to assess visually the relationship between the key climate variables,  
27 the data were normalised using statistical Z scores or standardised deviation scores  
28 (expressed as “Relative level” in the figures). In a Z-scored data series, each data  
29 point is part of an overall data series that sums to a zero mean and variance of 1,  
30 enabling comparison of data having different native units. Hence, when several Z-  
31 scored time series are depicted in a graph, all the time series will closely superimpose,  
32 enabling visual inspection to clearly discern the degree of similarity or dissimilarity  
33 between them.

1 See the individual figure legends for details on the series lengths.

2

3 In the time series analyses, SOI and global atmospheric surface temperature are the  
4 dependent variables. We tested the relationship between each of these variables and (1)  
5 the change in atmospheric CO<sub>2</sub> and (2) the variability in its rate of change. We  
6 express these CO<sub>2</sub>-related variables as finite differences. The finite differences used  
7 here are of both the first- and second-order types (we label these “first” and “second”  
8 differences in the text). Variability is explored using both intra-annual (monthly) data  
9 and interannual (yearly) data. The period covered in the figures is shorter than that  
10 used in the data preparation because of the loss of some data points due to calculations  
11 of differences and of moving averages (in monthly terms of up to 13 x 13), which  
12 commenced in January 1960.

13

14 Smoothing methods are used to the degree needed to produce similar amounts of  
15 smoothing for each data series in any given comparison. Notably, to achieve this  
16 outcome, series resulting from higher levels of differences require more smoothing.  
17 Smoothing is carried out initially by means of a 13-month moving average – this also  
18 minimises any remaining seasonal effects. If further smoothing is required, then this is  
19 achieved by taking a second moving average of the initial moving average (to  
20 produce a double moving average) (Hyndman 2010). Often, this is performed by  
21 means of a further 13 month moving average to produce a 13 x 13 moving average.  
22 For descriptive statistics to describe the long-term variation of a time series trend,  
23 polynomial smoothing is sometimes used.

24 It is important to consider what effects this filtering of our data may have on the  
25 ensuing statistical analysis. In these analyses, only the CO<sub>2</sub> series was smoothed and  
26 therefore requires assessment. To do this, we tested if the smoothed (2 x 13 month  
27 moving average) first-difference CO<sub>2</sub> series used here has different key dynamics to  
28 that of the original raw (unsmoothed) data from which the smoothed series was  
29 derived. Lagged correlogram analysis showed that the maximum, and statistically  
30 significant, correlation of the smoothed series with the unsmoothed series occurs  
31 when there is no phase shift. This suggests that the particular smoothing used should  
32 provide no problems in the assessment of which of first-difference CO<sub>2</sub> and  
33 temperature has priority.

1 Second, there is extensive evidence that while the effect that seasonal adjustment (via  
2 smoothing) on the usual tests for unit roots in time-series data is to reduce their power  
3 in small samples, this distortion is *not* an issue with samples of the size used in this  
4 study (see, e.g., Ghysels (1990), Frances (1991), Ghysels and Perron (1993), and  
5 Diebold (1993)). Moreover, Olekalns (1994) shows that seasonal adjustment by using  
6 dummy variables also impacts adversely on the finite-sample power of these tests, so  
7 there is little to be gained by considering this alternative approach. Finally, one of the  
8 results emerging from the Granger causality literature is that while such causality can  
9 be “masked” by the smoothing of the data, apparent causality cannot be “created”  
10 from non-causal data. For example, see Sims (1971), Wei (1982), Christiano and  
11 Eichenbaum (1987), Marcellino (1999), Breitung and Swanson (2002), and  
12 Gulasekaran and Abeysinghe (2002).

13 Finally, seasonally adjusting the data by a range of alternative approaches did not  
14 qualitatively change the results discussed in the paper. The results of these  
15 assessments are given in the Supplement.

16 This means that our results relating to the existence of Granger causality should not be  
17 affected adversely by the smoothing of the data that has been undertaken.

18  
19 Variables are led or lagged relative to one another to achieve best fit. These leads or  
20 lags were determined by means of time-lagged correlations (correlograms). The  
21 correlograms were calculated by shifting the series back and forth relative to each  
22 other, 1 month at a time.

23  
24 With this background, the convention used in this paper for unambiguously labelling  
25 data series and their treatment after smoothing or leading or lagging is depicted in the  
26 following example. The atmospheric CO<sub>2</sub> series is transformed into its second  
27 difference and smoothed twice with a 13 month moving average. The resultant series  
28 is then Z-scored. This is expressed as Z2x13mma2ndDerivCO<sub>2</sub>.

29  
30 Note that, to assist readability in text involving repeated references, atmospheric CO<sub>2</sub>  
31 is sometimes referred to simply as CO<sub>2</sub> and global surface temperature as temperature.

32

1 The time series methodology used in this paper involves the following procedures.  
2 First, any two or more time series being assessed by time series regression analysis  
3 must be what is termed stationary in the first instance, or be capable of being made  
4 stationary (by differencing). A series is stationary if its properties (mean, variance,  
5 covariances) do not change with time (Greene 2012). The (augmented) Dickey-Fuller  
6 test is applied to each variable. For this test, the null hypothesis is that the series has a  
7 unit root, and hence is non-stationary. The alternative hypothesis is that the series is  
8 integrated of order zero.

9  
10 Second, the residuals from any time series regression analysis then conducted must  
11 not be significantly different from white noise. This is done seeking correct model  
12 specification for the analysis.

13  
14 After Greene (2012): the results of standard ordinary least squares (OLS) regression  
15 analysis assume that the errors in the model are uncorrelated. Autocorrelation of the  
16 errors violates this assumption. This means that the OLS estimators are no longer the  
17 Best Linear Unbiased Estimators (BLUE). Notably and importantly this does not bias  
18 the OLS coefficient estimates. However statistical significance can be overestimated,  
19 and possibly greatly so, when the autocorrelations of the errors at low lags are positive.

20  
21 Addressing autocorrelation can take either of two alternative forms: *correcting for it*  
22 (for example, for first order autocorrelation by the Cochrane-Orcutt procedure), or  
23 *taking it into account*.

24  
25 In the latter approach, the autocorrelation is taken to be a consequence of an  
26 inadequate specification of the temporal dynamics of the relationship being  
27 estimated. The method of dynamic modelling (Pankratz 1991) addresses this by  
28 seeking to explain the current behavior of the dependent variable in terms of both  
29 contemporaneous and past values of variables. In this paper the dynamic modelling  
30 approach is taken.

31  
32 To assess the extent of autocorrelation in the residuals of the initial non-dynamic OLS  
33 models run, the Breusch-Godfrey procedure is used. Dynamic models are then used to  
34 take account of such autocorrelation. To assess the extent to which the dynamic

1 models achieve this, Kiviet's Lagrange multiplier F-test (LMF) statistic for  
2 autocorrelation (Kiviet 1986) is used.

3

4 Hypotheses related to Granger causality (see Introduction) are tested by estimating a  
5 multivariate time series model, known as a vector autoregression (VAR), for level of  
6 and first-difference CO<sub>2</sub> and other relevant variables. The VAR models the current  
7 values of each variable as a linear function of their own past values and those of the  
8 other variables. Then we test the hypothesis that  $x$  does not cause  $y$  by evaluating  
9 restrictions that exclude the past values of  $x$  from the equation for  $y$  and vice versa.

10 Stern and Kander (2011) observe that Granger causality is not identical to causation in  
11 the classical philosophical sense, but it does demonstrate the likelihood of such  
12 causation or the lack of such causation more forcefully than does simple  
13 contemporaneous correlation. However, where a third variable,  $z$ , drives both  $x$  and  $y$ ,  
14  $x$  might still appear to drive  $y$  though there is no actual causal mechanism directly  
15 linking the variables (any such third variable must have some plausibility - see  
16 Discussion and Conclusions below).

17

## 18 **4 Results**

19

### 20 **4.1. Relationship between first-difference CO<sub>2</sub> and temperature**

21

#### 22 **4.1.1. Priority**

23

24 Figure 2 showed that, while clearly first-difference CO<sub>2</sub> and temperature are not  
25 identical in signature, each is more alike than either is to the temperature model based  
26 on level of CO<sub>2</sub>. As well the figure shows that the same likeness relationships exist for  
27 the core trend. The purpose of the forthcoming sections is to see the extent to which  
28 these impressions are statistically significant.

29

30 The first question assessed is that of priority: which of first-difference atmospheric  
31 CO<sub>2</sub> and global surface temperature leads the other. The two series are shown for the  
32 period 1959 to 2012 in Figure 3.

33

34 To quantify the degree of difference in phasing between the variables, time-lagged  
35 correlations (correlograms) were calculated by shifting the series back and forth

1 relative to each other, one month at a time. These correlograms are given in Figure 4  
2 for global and regional data. For all four relationships shown, first-difference CO<sub>2</sub>  
3 always leads temperature. The leads differ as quantified in Table 1.

4  
5 It is possible for a lead to exist overall on average but for a lag to occur for one or  
6 other specific subsets of the data. This question is explored in Figure 5 and Table 2.  
7 Here the full 1959-2012 period of monthly data – some 640 months – for each of the  
8 temperature categories is divided into three approximately equal sub-periods, to  
9 provide 12 correlograms. It can be seen that in all 12 cases, first-difference CO<sub>2</sub> leads  
10 temperature. It is also noted that earlier sub-periods tend to display longer first-  
11 difference CO<sub>2</sub> leads. For the most recent sub-period the highest correlation is when  
12 the series are neither led nor lagged.

13  
14  
15

#### 16 **4.1.2 Correspondence between first-difference CO<sub>2</sub> and global surface** 17 **temperature curves**

18  
19

20 Next, the second prerequisite for causality, close correspondence, is also seen between  
21 first-difference CO<sub>2</sub> and global surface temperature in Figure 3.

22

#### 23 **4.1.3 Time series analysis**

24

25 Both first-difference CO<sub>2</sub> being shown to lead temperature, and the two series  
26 displaying close correspondence, are considered a firm basis for the time series  
27 analysis of the statistical relationship between first-difference CO<sub>2</sub> and temperature  
28 which follows. For this further analysis, we choose global surface temperature as the  
29 temperature series because, while its maximum correlation is not the highest (Figure  
30 5), its global coverage by definition is greatest. (In this section, TEMP stands for  
31 global surface temperature ((HadCRUT4), and other block capital terms are variable  
32 names used in the modelling).

33

34 The order of integration, denoted I(d), is an important characteristic of a time series. It  
35 reports the minimum number of differences required to obtain a covariance stationary  
36 series. As stated above, all series used in a time series regression must be series which

1 are stationary without further differencing (Greene 2012); that is, display an order of  
2 integration of  $I(0)$ . If a series has an order of integration greater than zero, it can be  
3 transformed by appropriate differencing into a new series which is stationary.

4  
5 By means of the Augmented Dickey–Fuller (ADF) test for unit roots, Table 3  
6 provides the information concerning stationarity for the level of, and first-difference  
7 of,  $CO_2$ , as well as for global surface temperature. Test results are provided for both  
8 monthly and annual data. The test was applied with an allowance for both a drift and  
9 deterministic trend in the data, and the degree of augmentation in the Dickey-Fuller  
10 regressions was determined by minimizing the Schwarz Information Criterion.

11  
12 The results show that for both the monthly and annual series used, the variables  
13 TEMP and FIRST-DIFFERENCE  $CO_2$  are stationary ( $I(0)$ ); but level of  $CO_2$  is not.  
14 Level of  $CO_2$  is shown to be  $I(1)$  because (Table 3) its first-difference is stationary .  
15 In contrast, Beenstock et al. (2012), using annual data, report that their series for the  
16 level of atmospheric  $CO_2$  forcing is an  $I(2)$  variable and therefore is stationary in  
17 *second* differences. To reconcile these two results, we refer to Pretis and Hendry  
18 (2013), who reviewed Beenstock et al. (2012). Pretis and Hendry (2013) take issue  
19 with the finding of  $I(2)$  for the anthropogenic forcings studied – including  $CO_2$  – and  
20 find evidence that this finding results from the combination of two different data sets  
21 measured in different ways which make up the 1850-2011 data set which Beenstock  
22 et al. test. Regarding this composite series Pretis and Hendry (2013) write:

23  
24 In the presence of these different measurements exhibiting structural changes,  
25 a unit-root test on the entire sample could easily not reject the null hypothesis  
26 of  $I(2)$  even when the data are in fact  $I(1)$ . Indeed, once we control for these  
27 changes, our results contradict the findings in Beenstock et al. (2012).

28  
29 Pretis and Hendry (2013) give their results for  $CO_2$  in their Table 1. Note that, in the  
30 table, level of  $CO_2$  data is transformed into first-difference data (Beenstock et al claim  
31 the *level* of  $CO_2$  is  $I(2)$ ); if that is the case, the first-difference of the level of  $CO_2$  Pretis  
32 and Hendry (2013) should find would be  $I(1)$  ).

33  
34 Pretis and Hendry (2013) state:

1  
2  
3  
4  
5  
6  
7  
8  
9  
10  
11  
12  
13  
14  
15  
16  
17  
18  
19  
20  
21  
22  
23  
24  
25  
26  
27  
28  
29  
30  
31  
32  
33

Unit-root tests are used to determine the level of integration of time series. Rejection of the null hypothesis provides evidence against the presence of a unit-root and suggests that the series is  $I(0)$  (stationary) rather than  $I(1)$  (integrated).

...based on augmented Dickey–Fuller (ADF) tests (see Dickey and Fuller, 1981), the first-difference of annual radiative forcing of  $CO_2$  is stationary initially around a constant (over 1850–1957), then around a linear trend (over 1958–2011). Although these tests are based on sub-samples corresponding to the shift in the measurement system, there is sufficient power to reject the null hypothesis of a unit root.

Hence for annual data Pretis and Hendry (2013) find first-difference  $CO_2$  to be stationary –  $I(0)$ , not  $I(1)$  – as is found in this study (Table 3).

With this question of the order of integration of the time series considered, we now turn to the next step of the time series analysis. As Table 3, above, and Pretis and Hendry (2013) show, the variable of the level of  $CO_2$  is non-stationary (specifically, integrated of order one, i.e.,  $I(1)$ ). Attempting to assess TEMP in terms of the level of  $CO_2$  would result in an “unbalanced regression”, as the dependent variable (TEMP) and the explanatory variable ( $CO_2$ ) have different orders of integration. It is well known (e.g., Banerjee et al. 1993, pp. 190-191, and the references therein) that in unbalanced regressions the t-statistics are biased away from zero. That is, one can appear to find statistically significant results when in fact they are not present. In fact, this occurrence of spurious significance is found when we regress TEMP on  $CO_2$ . This is strong evidence that any analysis should involve the variables TEMP and FIRST-DIFFERENCE  $CO_2$ , and not TEMP and  $CO_2$ .

For TEMP and FIRST-DIFFERENCE  $CO_2$ , one must next assess the extent to which autocorrelation affects the time series model. This is done by obtaining diagnostic statistics from an OLS regression. This regression shows, by means of the Breusch-Godfrey test for autocorrelation (up to order 12 – that is, including all monthly lags up to 12 months), that there is statistically significant autocorrelation at lags of one and

1 two months, leading to an overall Breusch-Godfrey Test statistic (LMF) = 126.901,  
2 with p-value =  $P(F(12,626) > 126.901) = 1.06 \times 10^{-158}$ .

3

4 Autocorrelation is a consequence of an inadequate specification of the temporal  
5 dynamics of the relationship being estimated. With this in mind, a dynamic model  
6 (Greene 2012) with two lagged values of the dependent variable as additional  
7 independent variables has been estimated. Results are shown in Table 4. The LMF  
8 test shows that there is now no statistically significant unaccounted-for  
9 autocorrelation, thus supporting the use of this dynamic model specification. Table 4  
10 shows that a highly statistically significant model has been established. First it shows  
11 that the temperature in a given period is strongly influenced by the temperature of  
12 closely preceding periods (see Discussion for a possible mechanism for this). Further,  
13 it provides evidence that there is also a clear, highly statistically significant role in the  
14 model for first-difference CO<sub>2</sub>.

15

16

#### 17 **4.1.4 Granger causality analysis**

18

19 We now can turn to assessing if first-difference atmospheric CO<sub>2</sub> may not only  
20 correlate with, but also contribute causatively to, global surface temperature. This is  
21 done by means of Granger causality analysis.

22

23 Recalling that both TEMP and FIRST-DIFFERENCE CO<sub>2</sub> are stationary, it is  
24 appropriate to test the null hypothesis of no Granger causality from FIRST-  
25 DIFFERENCE CO<sub>2</sub> to TEMP by using a standard Vector Autoregressive (VAR)  
26 model without any transformations to the data. The Akaike Information Criterion  
27 (AIC) and the Schwartz Information Criterion (SIC) were used to select an optimal  
28 maximum lag length (k) for the variables in the VAR. This lag length was then  
29 lengthened, if necessary, to ensure that:

30

31 (i) The estimated model was dynamically stable (i.e., all of the inverted roots  
32 of the characteristic equation lie inside the unit circle);

33 (ii) The errors of the equations were serially independent.

34

1  
2 The relevant EViews output from the VAR model is entitled VAR Granger  
3 Causality/Block Exogeneity Wald Tests and documents the following summary  
4 results – Wald Statistic (p-value): Null is there is No Granger Causality from FIRST-  
5 DIFFERENCE CO<sub>2</sub> to TEMP; Number of lags K=4; Chi-Square 26.684 (p-value =  
6 0.000). A p-value of this level is highly statistically significant and means the null  
7 hypothesis of No Granger Causality is very strongly rejected. That is, over the period  
8 studied there is strong evidence that FIRST-DIFFERENCE CO<sub>2</sub> Granger-causes  
9 TEMP.

10  
11 Despite the lack of stationarity in the level of CO<sub>2</sub> time series (meaning it cannot be  
12 used to model temperature), one can still assess the answer to the question: “Is there  
13 evidence of Granger causality between level of CO<sub>2</sub> and TEMP?”

14  
15 In answering this question, because the TEMP series is stationary, but the CO<sub>2</sub> series  
16 is non-stationary (it is integrated of order one,  $I(1)$ ), the testing procedure is modified  
17 slightly. Once again, the levels of both series are used. For each VAR model, the  
18 maximum lag length (k) is determined, but then one additional lagged value of both  
19 TEMP and CO<sub>2</sub> is included in each equation of the VAR. However, the Wald test for  
20 Granger non-causality is applied only to the coefficients of the original k lags of CO<sub>2</sub>.  
21 Toda and Yamamoto (1995) show that this modified Wald test statistic will still have  
22 an asymptotic distribution that is chi-square, even though the level of CO<sub>2</sub> is non-  
23 stationary. Here the relevant Wald Statistic (p-value): Null is there is No Granger  
24 Causality from level of CO<sub>2</sub> to TEMP; Number of lags K= 4; Chi-Square 2.531 (p-  
25 value = 0.470) . The lack of statistical significance in the p-value is strong evidence  
26 that level of CO<sub>2</sub> does not Granger-cause TEMP.

27  
28 With the above two assessments done, it is significant that with regard to global  
29 surface temperature we are able to discount causality involving the level of CO<sub>2</sub>, but  
30 establish causality involving first-difference CO<sub>2</sub>.

31  
32  
33  
34  
35

## **4.2 Relationship between second-difference CO<sub>2</sub> and temperature and Southern Oscillation Index**

#### 1 **4.2.1 Priority and correspondence**

2  
3 Given the results of this exploration of correlations involving first-difference  
4 atmospheric CO<sub>2</sub>, the possibility of the correlation of second-difference CO<sub>2</sub> with  
5 climate variables is also explored. The climate variables assessed are global surface  
6 temperature and the Southern Oscillation Index (SOI). In this section, data is from the  
7 full period for which monthly instrumental CO<sub>2</sub> data is available, 1958 to the present.  
8 For this period, the series neither led nor lagged appear as follows (Figure 6). For the  
9 purpose of this figure, to facilitate depiction of trajectory, second-difference CO<sub>2</sub> (left  
10 axis) and SOI (right axis) are offset so that all four curves display a similar origin in  
11 1960.

12  
13 Figure 6 shows that, alongside the close similarity between first-difference CO<sub>2</sub> and  
14 temperature already demonstrated, there is a second apparent distinctive pairing  
15 between second-difference CO<sub>2</sub> and SOI. The figure shows that the overall trend,  
16 amplitude and phase – the signature – of each pair of curves is both matched within  
17 each pair and different from the other pair. The remarkable sorting of the four curves  
18 into two groups is readily apparent. Each pair of results provides context for the  
19 other – and highlights the different nature of the other pair of results.

20  
21  
22 Recalling that (even uncorrected for any autocorrelation) correlational data still holds  
23 information concerning regression coefficients, we initially use OLS correlations  
24 without assessing autocorrelation to provide descriptive statistics. Table 5 includes,  
25 without any phase-shifting to maximise fit, the six pairwise correlations arising from  
26 all possible combinations of the four variables other than with themselves. Here it can  
27 be seen that the two highest correlation coefficients (in bold in the table) are firstly  
28 between first-difference CO<sub>2</sub> and temperature, and secondly between second-  
29 difference CO<sub>2</sub> and SOI.

30  
31 In Table 6, phase shifting has been carried out to maximise fit (shifts shown in  
32 variable titles in the table). This results in an even higher correlation coefficient for  
33 second-difference CO<sub>2</sub> and SOI.

1 The link between all three variable realms – CO<sub>2</sub>, SOI and temperature – can be  
2 further observed in Figure 7 and Table 7. Figure 7 shows SOI, second-difference  
3 atmospheric CO<sub>2</sub> and first-difference temperature, each of the latter two series phase-  
4 shifted for maximum correlation with SOI (as in Table 5). Looking at priority, Table 6  
5 shows that maximum correlation occurs when second-difference CO<sub>2</sub> leads SOI. It is  
6 also noted that the correlation coefficients for the correlations between the curves  
7 shown in Table 6 have all converged in value compared to those shown in Table 5.

8  
9 Looking at the differences between the curves shown in Figure 7, two of the major  
10 departures between the curves coincide with volcanic aerosols – from the El Chichon  
11 volcanic eruption in 1982 and the Pinatubo eruption in 1992 (Lean and Rind 2009).  
12 With these volcanism-related factors taken into account, it is notable (when expressed  
13 in the form of the transformations in Figure 7) that the signatures of all three curves  
14 are so essentially similar that it is almost as if all three curves are different versions  
15 of – or responses to – the same initial signal.

16 So, a case can be made that first- and second-difference CO<sub>2</sub> and temperature and SOI  
17 respectively are all different aspects of the same process.

18  
19  
20

#### 21 **4.2.2 Time series analysis**

22

23 We now assess more formally the relationship between second-difference CO<sub>2</sub> and  
24 SOI. As for first-difference CO<sub>2</sub> and temperature above, stationarity has been  
25 established. Again, there is statistically significant autocorrelation at lags of one and  
26 two months, leading to an overall Breusch-Godfrey Test statistic (LMF) of 126.9,  
27 with p-value =  $P(F(12,626) > 126.901) = 1.06 \times 10^{-158}$ .

28 Table 8 shows the results of a dynamic model with the dependent variable used at  
29 each of the two lags as further independent variables; there is now no statistically  
30 significant autocorrelation which has not been accounted for.

31

32 As Table 8 shows, a highly statistically significant model has been established. As for  
33 temperature, it shows that the SOI in a given period is strongly influenced by the SOI  
34 of closely preceding periods. Again as for temperature, it provides evidence that there  
35 is a clear role in the model for second-difference CO<sub>2</sub>.

1 With this established, it is noted that while the length of series in the foregoing  
2 analysis was limited by the start date of the atmospheric CO<sub>2</sub> series (January 1958),  
3 high temporal resolution (monthly) SOI goes back considerably further, to 1877. This  
4 long period SOI series (for background see Troup (1965)) is that provided by the  
5 Australian Bureau of Meteorology, sourced here from the Science Delivery Division  
6 of the Department of Science, Information Technology, Innovation and the Arts,  
7 Queensland, Australia. As equivalent temperature data is also available (the global  
8 surface temperature series already used above (HadCRUT4) goes back as far as 1850),  
9 these two longer series are now plotted in Figure 8. Notable is the continuation of the  
10 striking similarity between the two signatures already shown in Figure 7 over this  
11 longer period.

12  
13 Turning to regression analysis, as previously the Breusch-Godfrey procedure shows  
14 that, for lags up to lag 12, the majority of autocorrelation is again restricted to the first  
15 two lags. Table 9 shows the results of a dynamic model with the dependent variable  
16 used at each of the two lags as further independent variables.

17  
18 In comparison with Table 8, the extended time series modelled in Table 9 shows a  
19 remarkably similar R-squared statistic: 0.466 compared with 0.477. By contrast, the  
20 partial regression coefficient for second-difference CO<sub>2</sub> has increased, to 0.14  
21 compared with 0.077. It is beyond the scope of this study, but the relationship of SOI  
22 and second-difference CO<sub>2</sub> means it is now possible to produce a proxy for monthly  
23 atmospheric CO<sub>2</sub> from 1877 – a date approximately 75 years prior to the start of the  
24 CO<sub>2</sub> monthly instrumental record in January 1958.

25  
26

### 27 **4.2.3 Granger causality analysis**

28

29 This section assesses whether second-difference CO<sub>2</sub> can be considered to Granger-  
30 cause SOI. This assessment is carried out using data for the period 1959 to 2012.

31

32 Results of stationarity tests for each series are given in Table 10. Each series is shown  
33 to be stationary. These results imply that we can approach the issue of possible

1 Granger causality by using a conventional VAR model, in the levels of the data, with  
2 no need to use a "modified" Wald test (as used in the Toda and Yamamoto (1995)  
3 methodology).

4  
5 Simple OLS regressions of SOI against separate lagged values of second-difference  
6 CO<sub>2</sub> (including an intercept) confirm the finding that the highest correlation is when a  
7 two-period lag is used.

8  
9 A 2-equation VAR model is needed for reverse-sign SOI and second-difference CO<sub>2</sub>.  
10 Using SIC, the optimal maximum lag length is found to be 2 lags. When the VAR  
11 model is estimated with this lag structure (Table 11), testing the null hypothesis that  
12 there is no serial correlation at lag order h, shows that there is evidence of  
13 autocorrelation in the residuals.

14  
15 This suggests that the maximum lag length for the variables needs to be increased.  
16 The best results (in terms of lack of autocorrelation) were found when the maximum  
17 lag length is 3. (Beyond this value, the autocorrelation results deteriorated  
18 substantially, but the conclusions below, regarding Granger causality, were not  
19 altered.)

20  
21 Table 12 shows that the preferred, 3-lag model, still suffers a little from  
22 autocorrelation. However, as we have a relatively large sample size, this will not  
23 impact adversely on the Wald test for Granger causality.

24  
25 The relevant EViews output from the VAR model is entitled VAR Granger  
26 Causality/Block Exogeneity Wald Tests and documents the following summary  
27 results – Wald Statistic (p-value): Null is there is No Granger Causality from second-  
28 difference CO<sub>2</sub> to sign-reversed SOI; Chi-Square 22.554 (p-value = 0.0001).

29 The forgoing Wald statistic shows that the null hypothesis is strongly rejected – in  
30 other words, there is very strong evidence of Granger Causality from second-  
31 difference CO<sub>2</sub> to sign-reversed SOI.

32  
33  
34

### 1 **4.3 Paleoclimate data**

2  
3 So far, the time period considered in this study has been pushed back in the  
4 instrumental data realm to 1877. If non-instrumental paleoclimate proxy sources are  
5 used, CO<sub>2</sub> data now at annual frequency can be taken further back. The following  
6 example uses CO<sub>2</sub> and temperature data. The temperature reconstruction used here  
7 commences in 1500 and is that of Frisia et al. (2003), derived from annually  
8 laminated speliotem (stalagmite) records. A second temperature record (Moberg et  
9 al. 2005) is from tree ring data. The atmospheric CO<sub>2</sub> record (Robertson et al. 2001) is  
10 from fossil air trapped in ice cores and from instrumental measurements. The trends  
11 for these series are shown in Figure 9.

12  
13 Visual inspection of the figure shows that there is a strong overall likeness in  
14 signature between the two temperature series, and between them and first-difference  
15 CO<sub>2</sub>. The similarity of signature is notably less with level of CO<sub>2</sub>. It can be shown  
16 that level of CO<sub>2</sub> is not stationary and, even with the two other series which are  
17 stationary, the strongly smoothed nature of the temperature data makes removal of the  
18 autocorrelation impossible. Nonetheless, noting that data uncorrected for  
19 autocorrelation still provides valid correlations (Greene 2012) – only the statistical  
20 significance is uncertain – it is simply noted that first-difference CO<sub>2</sub> displays a better  
21 correlation with temperature than level of CO<sub>2</sub> for each temperature series (Table 13).

### 22 23 24 25 **4.4 Normalized Difference Vegetation Index (NDVI)**

26  
27 Using the Normalized Difference Vegetation Index (NDVI) time series as a measure  
28 of the activity of the land biosphere, this section now investigates the land biosphere  
29 as a candidate mechanism for the issue, identified in the Introduction, of the  
30 increasing difference between the observed global surface temperature trend and that  
31 suggested by general circulation climate models.

32  
33 The trend in the terrestrial CO<sub>2</sub> sink is estimated annually as part of the assessment of  
34 the well-known global carbon budget (Le Quere et al. 2014). It is noted that there is a

1 risk of circular argument concerning correlations between the terrestrial CO<sub>2</sub> sink and  
2 interannual (first-difference) CO<sub>2</sub> because the terrestrial CO<sub>2</sub> sink is defined as the  
3 residual of the global carbon budget (Le Quere et al. 2014). By contrast, the  
4 Normalized Difference Vegetation Index (NDVI) involves direct (satellite-derived)  
5 measurement of terrestrial plant activity. For this reason and because, of the two series,  
6 only NDVI is provided in monthly form, we will use only NDVI in what follows.

#### 9 **4.4.1. Preparation of the global NDVI series used in this paper**

10  
11 Globally aggregated GIMMS NDVI data from the Global Land Cover Facility site is  
12 available from 1980 to 2006. This dataset is referred to here as NDVIG. Spatially  
13 disaggregated GIMMS NDVI data from the GLCF site is available from 1980 to the  
14 end of 2013. An analogous global aggregation of this spatially disaggregated GIMMS  
15 NDVI data – from 1985 to end 2013 – was obtained from the Institute of Surveying,  
16 Remote Sensing and Land Information, University of Natural Resources and Life  
17 Sciences, Vienna. This dataset is abbreviated to NDVIV.

18  
19 Pooling the two series enabled the longest time span of data aggregated at global level.  
20 The two series were pooled as follows. Figure 10 shows the appearance of the two  
21 series. Each series is Z-scored by the same common period of overlap (1985-2006).  
22 The extensive period of overlap can be seen, as can the close similarity in trend  
23 between the two series. The figure also shows that the seasonal adjustment  
24 smoothings vary between the two series. Seasonality was removed for the NDVIV  
25 series using the 13 month moving average smoothing used throughout this paper. This  
26 required two passes using the 13 month moving average, which leads to a smoother  
27 result than seen for the NDVIG series.

28  
29 Pretis and Hendry (2013) observe that pooling data (i) from very different  
30 measurement systems and (ii) displaying different behaviour in the sub-samples can  
31 lead to errors in the estimation of the level of integration of the pooled series.

32  
33 The first risk of error (from differences in measurement systems) is overcome here as  
34 both the NDVI series are from the same original disaggregated data set. The risk

1 associated with the sub-samples displaying different behaviour and leading to errors  
2 in levels of integration is considered in the following section by assessing the order of  
3 each input series separately, and then the order of the pooled series.

4  
5 Table 14 provides order of integration test results for the three NDVI series. The  
6 analysis shows all series are stationary ( $I(0)$ ). It is, therefore, valid to pool the two  
7 series. Pooling was done by appending the Z-scored NDVIV data to the Z-scored  
8 NDVIG data at the point where the Z-scored NDVIG data ended (in the last month of  
9 2006).

10  
11 As discussed in the Introduction, Figure 1 shows that since around the year 2000 there  
12 is an increasing difference between the temperature projected by a mid-level IPCC  
13 model and that observed. Any cause for this increasing difference must itself show an  
14 increase in activity over this period.

15  
16 The purpose of this section is, therefore: (i) to derive an initial simple indicative  
17 quantification of the increasing difference between the temperature model and  
18 observation; and (ii) to assess whether global NDVI is increasing. If NDVI is  
19 increasing, this is support for NDVI being a candidate for the cause of the temperature  
20 model-observation difference. If there is a statistically significant relationship  
21 between the two increases, this is further support for NDVI being a candidate for the  
22 cause of the model-observation difference, and hence worthy of further detailed  
23 research. A full analysis of this question is beyond the scope of the present paper.

#### 24 25 26 **4.4.2 Preparation of the indicative series for the difference between the** 27 **temperature projected from a mid-level IPCC model and that observed**

28  
29 A simple quantification of the difference between the temperature projected from a  
30 mid-level IPCC model and that observed can be derived by subtracting the (Z-scored)  
31 temperature projected from the IPCC mid-range scenario model (CMIP3, SRESA1B  
32 scenario run for the IPCC fourth assessment report (IPCC 2007)) shown in Figure 1,  
33 from the observed global surface temperature also shown in Figure 1. This

1 quantification is depicted in Figure 13 for monthly data and, to reduce the influence of  
2 noise and seasonality, in Figure 14 for the same data pooled into three-year bins.

### 4 **4.4.3. Comparison of the pooled NDVI series with the difference between** 5 **projected and observed global surface temperature**

6  
7  
8 Figure 13, displaying monthly data, compares NDVI with the difference between the  
9 temperature projected from an IPCC mid-range scenario model (CMIP3, SRESA1B  
10 scenario run for the IPCC fourth assessment report (IPCC 2007)) and global surface  
11 temperature (red dotted curve). Both curves rise in more recent years.

12  
13 The trends for the 36-month pooled data in Figure 14 show considerable commonality.  
14 OLS regression analysis of the relationship between the curves in Figure 14 shows  
15 that the best fit between the curves involves no lead or lag. The correlation between  
16 the curves displays an adjusted R-squared value of 0.86. This is statistically  
17 significant ( $p = 0.00185$ ). As expected with such aggregated multi-year data, the  
18 relationship shows little or no autocorrelation (Test statistic:  $LMF = 1.59$  with  $p$ -value  
19  $= P(F(5,3) > 1.59) = 0.37$ ). The similarity between the trend in the NDVI and the  
20 difference between IPCC temperature modelling and observed temperature is  
21 evidence supporting the possibility that the NDVI may contribute to the observed  
22 global surface temperature departing from the IPCC modelling.

## 26 **5 Discussion**

27  
28  
29 The results in this paper show that there are clear links – at the highest standard of  
30 non-experimental causality — that of Granger causality — between first- and second-  
31 difference  $CO_2$  and the major climate variables of global surface temperature and the  
32 Southern Oscillation Index, respectively.

33  
34 Relationships between first- and second-difference  $CO_2$  and climate variables are  
35 present for all the time scales studied, including temporal start points situated as long  
36 ago as 1500. In the instances where time series analysis accounting for autocorrelation

1 could be successfully conducted, the results were always statistically significant. For  
2 the further instances (for those studies using data series commencing before 1877) the  
3 data was not amenable to time series analysis – and therefore also not amenable to  
4 testing for Granger causality – due to the strongly smoothed nature of the temperature  
5 data available which made removal of the autocorrelation impossible (see Section 4.3).  
6 Nonetheless, the scale of the non-corrected correlations observed was of the same  
7 order of magnitude as those of the instances that were able to be corrected for  
8 autocorrelation.

9

10 Given the time scales over which these effects are observed, the results taken as a  
11 whole clearly suggest that the mechanism observed is long term, and not, for example,  
12 a creation of the period of the steepest increase in anthropogenic CO<sub>2</sub> emissions, a  
13 period which commenced in the 1950s (IPCC 2014).

14 Taking autocorrelation fully into account in the time series analyses demonstrates the  
15 major role of immediate past instances of the dependent variable (temperature, and  
16 SOI) in influencing its own present state. This was found in all cases where time  
17 series models could be prepared. This was not to detract from the role of first- and  
18 second-difference CO<sub>2</sub> – in all relevant cases, they were significant in the models as  
19 well.

20

21 According to Wilks (1995) and Mudelsee (2010), such autocorrelation in the  
22 atmospheric sciences also called persistence or “memory” is characteristic for many  
23 types of climatic fluctuations.

24

25 In the specific case of the temperature and first-difference CO<sub>2</sub> relationship, the  
26 significant autocorrelation for temperature occurred with present temperature being  
27 affected by the immediately prior month and the month before that. As mentioned  
28 above, for atmospheric CO<sub>2</sub> and global surface temperature, others (Sun and Wang  
29 1996; Triacca 2005; Kodra et al. 2011; Attanasio and Triacca 2011; Attanasio 2012;  
30 Stern and Kaufmann 2014) have conducted Granger causality analyses involving the  
31 use of lags of both dependent and independent variables. These studies, however, are  
32 not directly comparable with the present study. Firstly, while reporting the presence or  
33 absence of Granger causality, the studies did not report lead or lag information.

1 Secondly, the studies used annual data, so could not investigate the dynamics of the  
2 relationships at the interannual (monthly) level where our findings were greatest.

3  
4 The anthropogenic global warming (AGW) hypothesis has two main dimensions  
5 (IPCC 2007; Pierrehumbert 2011): (i) that increasing CO<sub>2</sub> causes increasing  
6 atmospheric temperature (via a radiative forcing mechanism) and (ii) that most of the  
7 increase in atmospheric CO<sub>2</sub> in the last hundred years has been due to human causes.

8  
9 The results presented in this paper are supportive of the AGW hypothesis for two  
10 reasons: firstly, increasing atmospheric CO<sub>2</sub> is shown to drive increasing temperature;  
11 and secondly, the results deepen the evidence for a CO<sub>2</sub> influence on climate in that  
12 second-difference CO<sub>2</sub> is shown to drive the SOI.

13  
14 The difference between this evidence for the effect of CO<sub>2</sub> on climate and that of the  
15 standard AGW hypothesis is that the standard model proposes that temperature will  
16 rise roughly linearly with atmospheric CO<sub>2</sub>, whereas the present results show that the  
17 climate effects result from persistence of previous effects and from *rates of change* of  
18 CO<sub>2</sub>.

19  
20 On the face of it, then, this model seems to leave little room for the linear radiative  
21 forcing aspect of the AGW hypothesis.

22  
23 However more research is needed in this area.

24  
25 Reflection on Figure 1 shows that the radiative mechanism would be supported if a  
26 second mechanism existed to cause the difference between the temperature projected  
27 for the radiative mechanism and the temperature observed. The observed temperature  
28 would then be seen to result from the addition of the effects of these two mechanisms.

29  
30 As discussed in the Introduction, Hansen et al. (2013) have suggested that the  
31 mechanism for the pause in the global temperature increase since 1998 may be the  
32 planetary biota, in particular the terrestrial biosphere. As an initial indicative  
33 quantified characterisation of this possibility, Section 4.4 derived a simple measure of  
34 the increasing difference between the global surface temperature trend projected from

1 a mid-range scenario climate model and the observed trend. This depiction of the  
2 difference displayed a rising trend. The time series trend for the globally aggregated  
3 Normalized Difference Vegetation Index – which represents the changing levels of  
4 activity of the terrestrial biosphere – was also presented. This was shown also to  
5 display a rising trend.

6  
7 If by further research, for example by Granger causality analysis, the global  
8 vegetation can be shown to embody the second mechanism, this would be evidence  
9 that the observed global temperature does result from the effects of two mechanisms  
10 in operation together – the radiative, level-of-CO<sub>2</sub> mechanism, with the biological  
11 first-difference of CO<sub>2</sub> mechanism.

12  
13 Hence the biosphere mechanism would supplement, rather than replace, the radiative  
14 mechanism.

15  
16 Further comprehensive time series analysis of the NDVI data and relevant climate  
17 data, beyond the scope of the present paper, could throw light on these questions.

## 20 **References**

21  
22 Adams, J. M. and Piovesan, G.: Long series relationships between global interannual  
23 CO<sub>2</sub> increment and climate: Evidence for stability and change in role of the tropical  
24 and boreal-temperate zones. *Chemosphere*, 59, 1595 – 1612, 2005.

25  
26  
27 Attanasio, A. and Triacca, U.: Detecting human influence on climate using neural  
28 networks based Granger causality,” *Theor. Appl. Climatol.*, 103,1-2,103-107, 2011.

29  
30 Attanasio, A.: Testing for linear Granger causality from natural/anthropogenic  
31 forcings to global temperature anomalies *Theor. Appl. Climatol.* 110:281–289, 2012.

32  
33 Bacastow, R. B.: Modulation of atmospheric carbon dioxide by the southern  
34 oscillation, *Nature*, 261, 116–118, 1976.

35  
36 Banerjee, A. Dolado, J. Galbraith, J.W. and Hendry, D.F.: Co-integration, error-  
37 correction, and the econometric analysis of non-stationary data. Oxford University  
38 Press, Oxford, 1993.

39  
40 Barichivich, J., Briffa, K. R., Myneni, R. B., Osborn, T. J., Melvin, T. M., Ciais, P.,  
41 Piao, S., and Tucker, C.: Large-scale variations in the vegetation growing season and

1 annual cycle of atmospheric CO<sub>2</sub> at high northern latitudes from 1950 to 2011, *Glob.*  
2 *Change Biol.*, 19, 3167–3183, 2013.

3

4 Beenstock, M., Reingewertz, Y., and Paldor, N.: Polynomial cointegration tests of  
5 anthropogenic impact on global warming, *Earth Syst. Dynam.*, 3, 173–188,  
6 doi:10.5194/esd-3-173-2012, 2012.

7

8 Bellenger, H., Guilyardi, E., Leloup, J., Lengaigne, M., and Vialard, J.: ENSO  
9 representation in climate models: from CMIP3 to CMIP5, *Clim. Dynam.*, 42, 1999-  
10 2018, 2014.

11

12 Breitung, J. and Swanson, N. R.: Temporal aggregation and spurious instantaneous  
13 causality in multiple time series models. *Journal of Time Series Analysis*, 23, 651-665,  
14 2002.

15

16 Canty, T., Mascioli, N. R. Smarte, M. D. and Salawitch R. J. An empirical model of  
17 global climate – part 1: A critical evaluation of volcanic cooling, *Atmos. Chem. Phys.*  
18 13 3997–4031 2013.

19

20 Chen, X., and Tung, K. Varying planetary heat sink led to global-warming  
21 slowdown and acceleration. *Science* 345, 897, DOI: 10.1126/science.1254937, 2014.

22

23 Christiano, L. J. and Eichenbaum, M.: Temporal aggregation and structural inference  
24 in macroeconomics. *Carnegie-Rochester Conference Series on Public Policy*, 26, 63-  
25 130, 1987.

26

27

28 Denman, K.L., G. Brasseur, G. Chidthaisong, A. Ciais, P. P.M. Cox, P.M. Dickinson,  
29 R.E. Hauglustaine, D. Heinze, Holland, C.E, Jacob, D. Lohmann, U. Ramachandran,  
30 S. da Silva Dias, P.L. Wofsy, S.C. and Zhang, X.: Couplings between changes in the  
31 climate system and biogeochemistry, *Climate Change 2007: The physical science*  
32 *basis. Contribution of working group I to the fourth assessment report of the*  
33 *intergovernmental panel on climate change [Solomon, S. Qin, D. Manning, M. Chen,*  
34 *Z. MMarquis, M. Avery, K.B. Tignor, M. and Miller, H.L. (eds.)]. Cambridge*  
35 *University Press, Cambridge, United Kingdom and New York, NY, USA, 2007.*

36

37 Dickey, D.A. and Fuller, W.A.: Distribution of the estimators for autoregressive time  
38 series with a unit root, *Journal of the American Statistical Association*, 74, 427–431,  
39 1979.

40

41 Dickey, D. A. and Fuller, W. A.: Likelihood ratio statistics for autoregressive time  
42 series with a unit root, *Econometrica*, 49, 1057–1072, 1981.

43

44 Diebold, F. X.: Discussion: Effect of seasonal adjustment filters on tests for a unit  
45 root. *Journal of Econometrics*, 55, 99-103, 1993.

46 Dieleman, W. I. J. Vicca, S. Dijkstra, F. A. Hagedorn, F. Hovenden, M. J. Larsen, K.  
47 S. Morgan, J. A., Volder, A. Beier, C. Dukes, J. S. King, J. Leuzinger, S. Linder, S.  
48 Luo, Y. Oren, R. De Angelis, P. Tingey, D. Hoosbeek, M. R. and Janssens, I. A.  
49 Simple additive effects are rare: a quantitative review of plant biomass and soil

1 process responses to combined manipulations of CO<sub>2</sub> and temperature, *Glob. Change*  
2 *Biol.*, 18, 2681–2693, 2012.

3

4 Elliott, G., Rothenberg T. J., and Stock J. H.: Efficient tests for an autoregressive  
5 unit root, *Econometrica*, 64, 813-836, 1996.

6 Folland C.K., Colman A.W., Smith D.M., Boucher O., Parker D.E., and Vernier J.P. :  
7 High predictive skill of global surface temperature a year ahead, *Geophys. Res. Lett.*,  
8 40, 761–767, 2013.

9

10 Foster, G. and Rahmstorf, S.: Global temperature evolution 1979–2010, *Environ. Res.*  
11 *Lett.*, 6, 044022, 2011.

12

13 Franses, P. H.: Moving average filters and unit roots. *Economics Letters*, 37, 399-403.,  
14 1991.

15

16 Frisia, S., A. Borsato, N. Preto, and F. McDermott.: Late Holocene annual growth in  
17 three Alpine stalagmites records the influence of solar activity and the North Atlantic  
18 Oscillation on winter climate, *Earth and Planetary Science Letters*, 216, 411–424,  
19 2003.

20

21 Fyfe, J. C., Gillett, N.P, and Zwiers, F. W.: Overestimated global warming over the  
22 past 20 years, *Nature Climate Change*, 3 767–769, 2013.

23 Fyfe J.C and Gillett, N.P.: Recent observed and simulated warming, *Nature Climate*  
24 *Change*, 4, 150-151, 2014.

25

26 Ghysels, E.: Unit root tests and the statistical pitfalls of seasonal adjustment: The case  
27 of U.S. postwar real gross national product. *Journal of Business and Economic*  
28 *Statistics*, 8, 145-152, 1990.

29

30 Ghysels, E. and Perron, P.: The effect of seasonal adjustment filters on tests for a unit  
31 root. *Journal of Econometrics*, 55, 57-98, 1993.

32

33 Granger, C.W.J.: Investigating causal relations by econometric models and cross-  
34 spectral methods, *Econometrica*, 37, 3, 424-438, 1969.

35

36 Greene, W. H.: *Econometric Analysis* (7th ed.), Prentice Hall, Boston, 2012.

37

38 Gnu Regression, Econometrics and Time-Series Library. GRETL 1.7.5. Available  
39 from: <http://gretl.sourceforge.net/>[Accessed April 23, 2008

40

41 Gribbons, B. and Herman, J.: True and quasi-experimental designs. *Practical*  
42 *assessment, research and evaluation*, 5, <http://PAREonline.net/getvn.asp?v=5&n=14>,  
43 1997.

44

45 Guemas V., Doblas-Reyes F.J., Andreu-Burillo I. and Asif M.: Retrospective  
46 prediction of the global warming slowdown in the past decade, *Nature Climate*  
47 *Change*, 3, 649–653, 2013.

1  
2 Guilyardi, E., Bellenger H., Collins M., Ferrett S., Cai, W., and Wittenberg A.: A  
3 first look at ENSO in CMIP5, *Clivar. Exch.*, 17, 29–32, 2012.  
4  
5 Gulasekaran, R. and Abeysinghe, T.: The distortionary effects of temporal aggregation  
6 on Granger causality. Working Paper No. 0204, Department of Economics, National  
7 University of Singapore, 2002.  
8  
9 Ghosh, S. and Rao, C. R. eds.: Design and Analysis of Experiments, *Handbook of*  
10 *Statistics*, 13, North-Holland, 1996.  
11  
12 Hansen, J., Kharecha, P., and Sato, M.: Climate forcing growth rates: doubling down  
13 on our Faustian bargain, *Environ. Res. Lett.*, 8, 2013.  
14  
15 Hidalgo, F. and Sekhon, J.: Causality. In Badie, B., Berg-Schlosser, D., and Morlino,  
16 L. (Eds.), *International encyclopedia of political science*, 204-211, 2011.  
17  
18 Holbrook, N.J. Davidson, J. Feng, M. Hobday, A.J. Lough, J.M. McGregor, S. and  
19 Risbey, J.S.: El niño-southern oscillation, In: A marine climate change impacts and  
20 adaptation report card for Australia 2009, (Eds. Poloczanska, E.S. Hobday, A.J. and  
21 Richardson, A.J.) NCCARF Publication, 05/09, 2009.  
22  
23 Hume D.: An enquiry into human understanding (1751) cited in: Hidalgo, F., &  
24 Sekhon, J.: Causality. In Badie, B., Berg-Schlosser, D. & Morlino, L. (Eds.)  
25 *International encyclopedia of political science*, 204-211, 2011.  
26  
27 Hyndman, R.J.: Moving averages. in Lovirc, M. (ed.), *International encyclopedia of*  
28 *statistical science*. 866-869 Springer, New York, 2010.  
29  
30 IHS EViews: *EViews 7.2*, Irvine CA. , 2011.  
31  
32 Imbers, J., Lopez, A., Huntingford, C., and Allen M. R.: Testing the robustness of the  
33 anthropogenic climate change detection statements using different empirical models, *J.*  
34 *Geophys. Res.-Atmos.*, 118, 3192–3199, 2013.  
35  
36 IPCC: *Climate Change 2007: The physical science basis. Contribution of working*  
37 *group I to the fourth assessment report of the intergovernmental panel on climate*  
38 *change* [IPCC, Qin, D., Manning, M., Chen, Z., Marquis, M., Avery, K.B., Tignor, M.  
39 and Miller, H.L. (eds.)]. Cambridge University Press, Cambridge, United Kingdom  
40 and New York, NY, USA, 2007.  
41  
42 IPCC, 2014: *Climate Change 2013: The Physical Science Basis. Contribution of*  
43 *Working Group I to the Fifth Assessment Report of the Intergovernmental Panel on*  
44 *Climate Change* [Stocker, T.F., D. Qin, G.-K. Plattner, M. Tignor, S.K. Allen, J.  
45 Boschung, A. Nauels, Y. Xia, V. Bex and P.M. Midgley  
46 (eds.)]. Cambridge University Press, Cambridge, United Kingdom and New York, NY,  
47 USA, 1535 pp.  
48  
49 Kaufmann R.K., Kauppi H., and Stock J.H.: Emissions, concentrations, and  
50 temperature: a time series analysis, *Clim. Change*, 77, 249–278, 2006.

1  
2 Keeling R-F, Piper S-C, Bollenbacher A-F, Walker S-J (2009) Carbon Dioxide  
3 Research Group, Scripps Institution of Oceanography (SIO), University of California,  
4 La Jolla, California USA 92093-0444, Feb 2009.,  
5 <http://cdiac.ornl.gov/ftp/trends/co2/maunaloa.co2>, last access: 14 July 2014.  
6  
7 Kiviet, J.F.: On the rigour of some misspecification tests for modelling dynamic  
8 relationships, *Review of Economic Studies*, 53, 241-261, 1986.  
9  
10 Kodra, E., Chatterjee, S., and Ganguly, A.R.: Exploring Granger causality between  
11 global average observed time series of carbon dioxide and temperature, *Theoretical*  
12 *and Applied Climatology*, 104, 3-4, 325-335, 2011.  
13  
14 Kopp, G. and Lean, J. L.: A new, lower value of total solar irradiance: evidence and  
15 climate significance. *Geophys. Res. Lett.*, 38, 2011.  
16  
17 Kosaka, Y. and Shang-Ping, X.: Recent global-warming hiatus tied to equatorial  
18 Pacific surface cooling, *Nature*, doi:10.1038/nature12534, 2013.  
19  
20 Kuo C., Lindberg C., and Thomson D.J.: Coherence established between atmospheric  
21 carbon dioxide and global temperature, *Nature*, 343, 709–714, 1990.  
22 Kwiatkowski, D.; Phillips, P. C. B.; Schmidt, P. and Shin, Y.: Testing the null  
23 hypothesis of stationarity against the alternative of a unit root, *Journal of*  
24 *Econometrics* 54, 159–178, 1992.  
25  
26  
27 Le Quéré, C., Peters, G. P., Andres, R. J., Andrew, R. M., Boden, T., Ciais, P.,  
28 Friedlingstein, P., Houghton, R. A., Marland, G., Moriarty, R., Sitch, S., Tans, P.,  
29 Arneeth, A., Arvanitis, A., Bakker, D. C. E., Bopp, L., Canadell, J. G., Chini, L. P.,  
30 Doney, S. C., Harper, A., Harris, I., House, J. I., Jain, A. K., Jones, S. D., Kato,  
31 E., Keeling, R. F., Klein Goldewijk, K., Körtzinger, A., Koven, C., Lefèvre, N., Omar,  
32 A., Ono, T., Park, G.-H., Pfeil, B., Poulter, B., Raupach, M. R., Regnier, P.,  
33 Rödenbeck, C., Saito, S., Schwinger, J., Segschneider, J., Stocker, B. D., Tilbrook, B.,  
34 vanHeuven, S., Viovy, N., Wanninkhof, R., Wiltshire, A., Zaehle, S., and Yue, C.:  
35 Global carbon budget 2013, *Earth Syst. Sci. Data*, 6, 235–263, 2014  
36  
37 Lean, J.L. and Rind, D.H.: How natural and anthropogenic influences alter global and  
38 regional surface temperatures: 1889 to 2006, *Geophys. Res. Lett.*, 35, 2008.  
39  
40 Lean, J. L. and Rind, D.H.: How will Earth’s surface temperature change in future  
41 decades? *Geophys. Res. Lett.* 36, L15708, 2009.  
42  
43 Lean, J.L. and Rind, D.H.: How natural and anthropogenic influences alter global and  
44 regional surface temperatures: 1889 to 2006, *Geophys. Res. Lett.*, 35, 2008.  
45  
46 Lockwood M.: Recent changes in solar outputs and the global mean surface  
47 temperature. III. Analysis of contributions to global mean air surface temperature rise.

1 Proceedings of the Royal Society, Mathematical Physical and Engineering Sciences,  
2 464, 1387–1404, 2008.

3

4 Marcellino, M.: Some consequences of temporal aggregation in empirical  
5 analysis. *Journal of Business and Economic Statistics*, 17, 129-136, 1999.

6 Meehl, G. A. Arblaster, J.M. Fasullo, J.T.1, Hu, A, and Trenberth, K.E.: Model-based  
7 evidence of deep-ocean heat uptake during surface-temperature hiatus periods, *Nature*  
8 *Climate Change*, DOI: 10.1038/NCLIMATE1229, 2011.

9

10 Meehl, G. A., C. Covey, T. Delworth, M. Latif, B. McAvaney, J. F. B. Mitchell, R. J.  
11 Stouffer, and K. E. Taylor: The WCRP CMIP3 multi-model dataset: A new era in  
12 climate change research, *Bulletin of the American Meteorological Society*, **88**, 1383-  
13 1394. 2007. (CMIP3) Multi-Model Mean20c3m/sresa1,  
14 [http://climexp.knmi.nl/selectfield\\_CO2](http://climexp.knmi.nl/selectfield_CO2), last access 10 June 2014

15

16 Moberg, A., D.M. Sonechkin, K. Holmgren, N.M. Datsenko and W. Karlén.: Highly  
17 variable Northern Hemisphere temperatures reconstructed from low- and high-  
18 resolution proxy data, *Nature*, 433, 7026, 613-617, 2005.

19

20 Morice, C.P., Kennedy, J.J., Rayner, N.A. and Jones, P.D.: Quantifying uncertainties  
21 in global and regional temperature change using an ensemble of observational  
22 estimates: the HadCRUT4 dataset. *Journal of Geophysical Research*, **117**, 2012.  
23 D08101, [doi:10.1029/2011JD017187](https://doi.org/10.1029/2011JD017187)  
24 <http://www.metoffice.gov.uk/hadobs/hadcrut4/data/download.html>, last access 25  
25 August 2014.

26

27 Mudelsee, M.: *Climate Time Series Analysis*. Springer, 2010.

28

29 Ng, S. and Perron, P.: Lag length selection and the construction of unit root tests with  
30 good size and power, *Econometrica*, 69, 1519-1554, 2001.

31

32 Olekalns, N.: Testing for unit roots in seasonally adjusted data. *Economics Letters*, 45,  
33 273-279, 1994.

34 Pankratz, A.: *Forecasting with Dynamic Regression Models*. Wiley, 1991.

35

36

37 Pierrehumbert, R.: Infrared radiation and planetary temperature. *Physics Today*, 64,  
38 33–38, 2011.

39

40

41 Pretis, F. and Hendry, D. F.: Comment on “Polynomial cointegration tests of  
42 anthropogenic impact on global warming” by Beenstock et al. (2012) - some hazards  
43 in econometric modelling of climate change. *Earth System Dynamics* 4, 375–384,  
44 2013.

45

46 Phillips, P.C.B. and Perron, P.: Testing for a unit root in time series regression,  
47 *Biometrika*, 75, 335–346, 1988.

48

1 Robertson, A. Overpeck, J. Rind, D. Mosley-Thompson, D. E. Zielinski, G. Lean, J.  
2 Koch, D. Penner, J. Tegen, I. & Healy, R.: Hypothesized climate forcing time series  
3 for the last 500 years, *Journal of Geophysical Research*, 106, D14, 2001.  
4

5 Running, S. W., Nemani, R. R., Heinsch, F. A., Zhao, M., Reeves, M. C., and  
6 Hashimoto, H.: A continuous satellite-derived measure of global terrestrial primary  
7 production, *BioScience*, 54, 547–560, 2004  
8

9 Sato, M., Hansen, J. E., McCormick, M. P. & Pollack, J. B. Stratospheric aerosol  
10 optical depths, 1850–1990. *J. Geophys. Res.*, 98, 22987–22994, 1993.  
11 [http://data.giss.nasa.gov/modelforce/strataer/tau.line\\_2012.12.txt](http://data.giss.nasa.gov/modelforce/strataer/tau.line_2012.12.txt), last access 10  
12 August 2014.  
13

14 Stahle, D.W., R.D. D'Arrigo, P.J. Krusic, M.K. Cleaveland, E.R. Cook,  
15 R.J. Allan, J.E. Cole, R.B. Dunbar, M.D. Therrell, D.A. Gay, M.D. Moore,  
16 M.A. Stokes, B.T. Burns, J. Villanueva-Diaz and L.G. Thompson: Experimental  
17 dendroclimatic reconstruction of the Southern Oscillation. *Bull. American*  
18 *Meteorological Society* 79: 2137-2152, 1998.  
19

20 Stern, D.I. and Kander, A.: The role of energy in the industrial revolution and modern  
21 economic growth, CAMA Working Paper Series, Australian National University,  
22 2011.  
23

24 Stern, D.I and Kaufmann, R.K.: Anthropogenic and natural causes of climate change,  
25 *Climatic Change*, 122, 257-269, DOI 10.1007/s10584-013-1007-x, 2014.  
26

27 Sun, L. and Wang, M.: Global warming and global dioxide emission: an empirical  
28 study, *Journal of Environmental Management*, 46, 327–343, 1996.  
29

30 Thornton, D. L. and Batten, D. S.: Lag-length selection and tests of Granger causality  
31 between money and income. *Journal of Money, Credit and Banking*, 17, 164-178,  
32 1985.

33 Toda, H. Y. and Yamamoto, T.: Statistical inferences in vector autoregressions with  
34 possibly integrated processes, *Journal of Econometrics*, 66, 225-250. 1995.  
35

36 Triacca, U.: Is Granger causality analysis appropriate to investigate the relationship  
37 between atmospheric concentration of carbon dioxide and global surface air  
38 temperature?, *Theoretical and Applied Climatology*, 81, 133–135, 2005.  
39

40 Troup, A.J.: The Southern Oscillation, *Quarterly Journal of Royal Meteorological*  
41 *Society*, 91, 490-506, 1965.  
42 [https://www.longpaddock.qld.gov.au/seasonalclimateoutlook/southernoscillationindex](https://www.longpaddock.qld.gov.au/seasonalclimateoutlook/southernoscillationindex/soidatafiles/MonthlySOI1887-1989Base.txt)  
43 [/soidatafiles/MonthlySOI1887-1989Base.txt](https://www.longpaddock.qld.gov.au/seasonalclimateoutlook/southernoscillationindex/soidatafiles/MonthlySOI1887-1989Base.txt), last access 25 August 2014.  
44

45 Tucker, C.J., J. E. Pinzon, M. E. Brown, D. Slayback, E. W. Pak, R. Mahoney, E.  
46 Vermote and N. El Saleous, An extended AVHRR 8-km NDVI data set compatible  
47 with MODIS and SPOT vegetation NDVI data, *International Journal of Remote*  
48 *Sensing*, 26, 4485-5598, 2005.

1 <http://climexp.knmi.nl/select.cgi?id=someone@somewhere&field=ndvi>, last access  
2 30 July 2014.

3  
4 Tung, K.-K. and Zhou, J.: Using data to attribute episodes of warming and cooling in  
5 instrumental records, PNAS, 110, 2058-2063, 2013.

6  
7 Wang, C., Deser, C., Yu, J.-Y., DiNezio, P., and Clement, A.: El Niño–Southern  
8 Oscillation (ENSO): a review, in: Coral Reefs of the Eastern Pacific, Glynn, P.  
9 Manzello, D., and Enochs, I., Springer Science, 2012.

10  
11 Wang, W., Ciais, P., Nemani, R. R., Canadell, J. G., Piao, S., Sitch, S., White, M. A.,  
12 Hashimoto, H., Milesi, C., and Myneni, R. B.: Variations in atmospheric CO<sub>2</sub> growth  
13 rates coupled with tropical temperature, Proc. Natl. Acad. Sci. USA, 110, 13061–  
14 13066, 2013.

15  
16 Wei, W. W. S.: The effect of systematic sampling and temporal aggregation on  
17 causality – a cautionary note. Journal of the American Statistical Association, 77, 316-  
18 319, 1982.

19  
20 Wilks, D.S.: Statistical methods in the atmospheric sciences: an introduction.  
21 Academic Press; 2011.

22  
23 Zhang, Y., Guanter, L., Berry J.A., Joiner, J., van der Tol, C., Huete, A., Gitelson,  
24 A., Voigt, M., and Köhler P.: Estimation of vegetation photosynthetic capacity from  
25 space-based measurements of chlorophyll fluorescence for terrestrial biosphere  
26 models, Global Change Biology, doi: 10.1111/gcb.12664, 2014.

27  
28 Zhou, J. and Tung, K.: Deducing multidecadal anthropogenic global warming trends  
29 using multiple regression analysis, Journal of the Atmospheric Sciences, 70, 1-8,  
30 2013.

31  
32  
33

34

35

36

37

38

39

40

41

1  
2  
3  
4  
5  
6  
7  
8  
  
9  
10  
11  
12  
13  
14  
15  
16  
17  
18  
19  
20  
21

**Table 1.** Lag of first-difference CO<sub>2</sub> relative to surface temperature series for global, tropical, northern hemisphere and southern hemisphere categories

	<b>Lag in months of first-difference CO<sub>2</sub> relative to global surface temperature category</b>
<b>Hadcrut4SH</b>	-1
<b>Hadcrut4Trop</b>	-1
<b>Hadcrut4_nh</b>	-3
<b>Hadcrut4Glob</b>	-2

1

2

3

4 **Table 2.** Lag of FIRST-DIFFERENCE CO<sub>2</sub> relative to surface temperature series for  
5 global, tropical, northern hemisphere and southern hemisphere categories, each for  
6 three time-series sub-periods

Temperature category	Time period	Lag of first-difference CO <sub>2</sub> relative to global surface temperature series
NH	1959.87 to 1976.46	-6
NH	1976.54 to 1993.21	-6
Global	1959.87 to 1976.46	-4
SH	1959.87 to 1976.46	-3
Global	1976.54 to 1993.21	-2
Tropical	1959.87 to 1976.46	0
Tropical	1976.54 to 1993.21	0
Tropical	1993.29 - 2012.37	0
Global	1993.29 - 2012.37	0
NH	1993.29 - 2012.37	0
SH	1976.54 to 1993.21	0
SH	1993.29 - 2012.37	0

7

8

9

10

11

1  
2  
3  
4  
5  
6  
7  
8  
9  
10

**Table 3.** Augmented Dickey–Fuller (ADF) test for tests for unit roots stationarity in both monthly and annual data 1969 to 2012 for, level of atmospheric CO<sub>2</sub>, first-difference CO<sub>2</sub> and global surface temperature

	Monthly data				Annual data			
	ADF statistic*	p-value	Order of integration	Test interpretation	ADF statistic*	p-value	Order of integration	Test interpretation
Level of CO <sub>2</sub>	-0.956	0.9481	I(1)	Non-stationary	-0.309	0.991	I(1)	Non-stationary
First-Difference CO <sub>2</sub>	-17.103	5.72 E-54	I(0)	Stationary	-4.319	0.003	I(0)	Stationary
Temp	-5.115	0.00011	I(0)	Stationary	-3.748	0.019	I(0)	Stationary

11 \* The Dickey-Fuller regressions allowed for both drift and trend; the augmentation level  
12 was chosen by minimizing the Schwarz Information Criterion.

13  
14  
15  
16  
17  
18

**Table 4.** OLS dynamic regression between first-difference atmospheric CO<sub>2</sub> and global surface temperature for monthly data for the period 1959 - 2012, with autocorrelation taken into account

Independent variable/s [1]	Dependent variable [1]	Independent variable regression coefficients	Independent variable P-value	Whole model adjusted R-squared	Whole model P-value	LM test for autocorrelation [2]
Led2mx13mma 1stderiv CO <sub>2</sub>	TEMP	0.097	<0.00001	0.861	6.70E-273	0.144
Led1mTEMP		0.565	<0.00001			
Led2mTEMP		0.306	<0.00001			

19 [1] Z-scored  
20 [2] Whole model: LM test for autocorrelation up to order 12 - Null hypothesis: no autocorrelation  
21

22

1  
2  
3  
4  
5  
6

**Table 5.** Pairwise correlations (correlation coefficients (R)) between selected climate variables

	<b>2x13mmafirstderiv CO<sub>2</sub></b>	<b>Hadcrut4Global</b>	<b>3x13mma2ndderivCO<sub>2</sub></b>
Hadcrut4Global	<b>0.7</b>	1	
3x13mma2ndderivCO <sub>2</sub>	0.06	-0.05	1
13mmaReverseSOI	0.25	0.14	<b>0.37</b>

7  
8  
9

**Table 6.** Pairwise correlations (correlation coefficients (R)) between selected climate variables, phase-shifted as shown in the table

	<b>Led2m2x13mmafirstderivCO<sub>2</sub></b>	<b>Hadcrut4Global</b>	<b>Led4m3x13mma2ndderivCO<sub>2</sub></b>
Hadcrut4Global	<b>0.71</b>	1	
Led4m3x13mma2nddiffCO <sub>2</sub>	0.23	0.09	1
13mmaReverseSOI	0.16	0.14	<b>0.49</b>

13  
14  
15  
16  
17

**Table 7.** Pairwise correlations (correlation coefficients (R)) between selected climate variables, phase-shifted as shown in the table

	<b>ZLed2m2x13mma2ndderivCO<sub>2</sub></b>	<b>ZReverseSOI</b>
ZReverseSOI	0.28	1.00
ZLed3m13mmafirstdiffhadcrut4global	0.35	0.41

18  
19  
20  
21  
22  
23

**Table 8.** OLS dynamic regression between second-difference atmospheric CO<sub>2</sub> and reversed Southern Oscillation Index for monthly data for the period 1959 - 2012, with autocorrelation taken into account

<b>Independent variable/s [1]</b>	<b>Dependent variable [1]</b>	<b>Independent variable regression coefficients</b>	<b>Independent variable P-value</b>	<b>Whole model adjusted R-squared</b>	<b>Whole model P-value</b>	<b>LM test for autocorrelation [2]</b>

Led3m2x13mma 1stderivCO <sub>2</sub>	ReverseSOI	0.07699	<0.011	0.478	1.80E- 89	0.214
Led1mReverseSOI		0.456	<0.00001			
Led2mreverseSOI		0.272	<0.00001			

[1] Z-scored

[2] Whole model: LM test for autocorrelation up to order 12 - Null hypothesis: no autocorrelation

Table 9. OLS dynamic regression between first-difference global surface temperature and reversed Southern Oscillation Index for monthly data for the period 1877-2012, with autocorrelation taken into account

Indep-endent variable/s [1]	Dep-endent variable [1]	Independent variable regression coefficients	Indep-endent variable P-value	Whole model adjusted R-squared	Whole model P-value	LM test for autocorr-elation [2]
Led3m12mma1stdiffTEMP	ReverseSOI	0.140	<0.00001	0.466	3.80E- 221	0.202
Led1mReverseSOI		0.465	<0.00001			
Led2mReverseSOI		0.210	<0.00001			

[1] Z-scored

[2] Whole model: LM test for autocorrelation up to order 3 - Null hypothesis: no autocorrelation

Table 10: Augmented Dickey–Fuller (ADF) test for stationarity for monthly data 1959 to 2012 for second-difference CO<sub>2</sub> and sign-reversed SOI

	ADF statistic	p-value	Test interpretation
Second-difference CO <sub>2</sub>	-10.077	0.000	Stationary
Sign-reversed SOI	-6.681	0.000	Stationary

Table 11. VAR Residual Serial Correlation LM Tests component of Granger causality testing of relationship between second-difference CO<sub>2</sub> and SOI. Initial 2-lag model

Lag order	LM-Stat	P-value*
1	10.62829	0.0311
2	9.71675	0.0455
3	2.948737	0.5664
4	9.711391	0.0456
5	10.67019	0.0305
6	37.13915	0
7	1.268093	0.8668

\*P-values from chi-square with 4 df.

1  
2  
3  
4  
5

**Table 12.** VAR Residual Serial Correlation LM Tests component of Granger causality testing of relationship between second-difference CO<sub>2</sub> and SOI. Preferred 3-lag model

Lag order	LM-Stat	P-value*
1	1.474929	0.8311
2	4.244414	0.3739
3	2.803332	0.5913
4	13.0369	0.0111
5	8.365221	0.0791
6	40.15417	0
7	1.698265	0.791

\*P-values from chi-square with 4 df.

6  
7  
8  
9

**Table 13.** Correlations (R) between paleoclimate CO<sub>2</sub> and temperature estimates 1500-1940

	Temperature (speliotherm)	Temperature (tree ring)
Level of CO <sub>2</sub> (ice core)	0.369	0.623
1st diff. CO <sub>2</sub> (ice core)	0.558	0.721

10  
11  
12  
13  
14  
15  
16

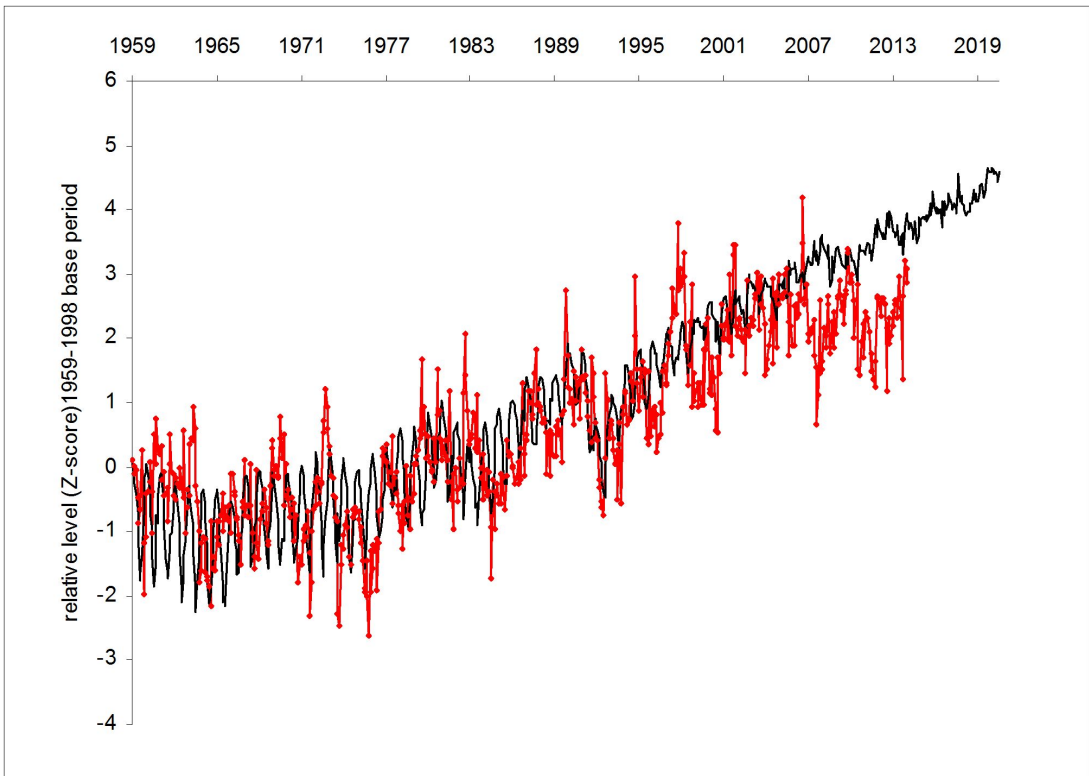
**Table 14.** Order of integration test results for NDVI series for monthly data from 1981-2012. The Schwartz Information Criterion (SIC) was used to select an optimal maximum lag length in the tests.

NDVI Series	Null Hypothesis: the series has a unit root	Probability of unit root
NDVIV	Lag Length: 16 (Automatic - based on SIC, maxlag=16)	0.0122
NDVIG	Lag Length: 1 (Automatic - based on SIC, maxlag=15)	7.23e-14
NDVIGV	Lag Length: 1 (Automatic - based on SIC, maxlag=16)	4.18E-16

17  
18  
19  
20  
21  
22

1  
2  
3  
4  
5  
6  
7  
8  
9

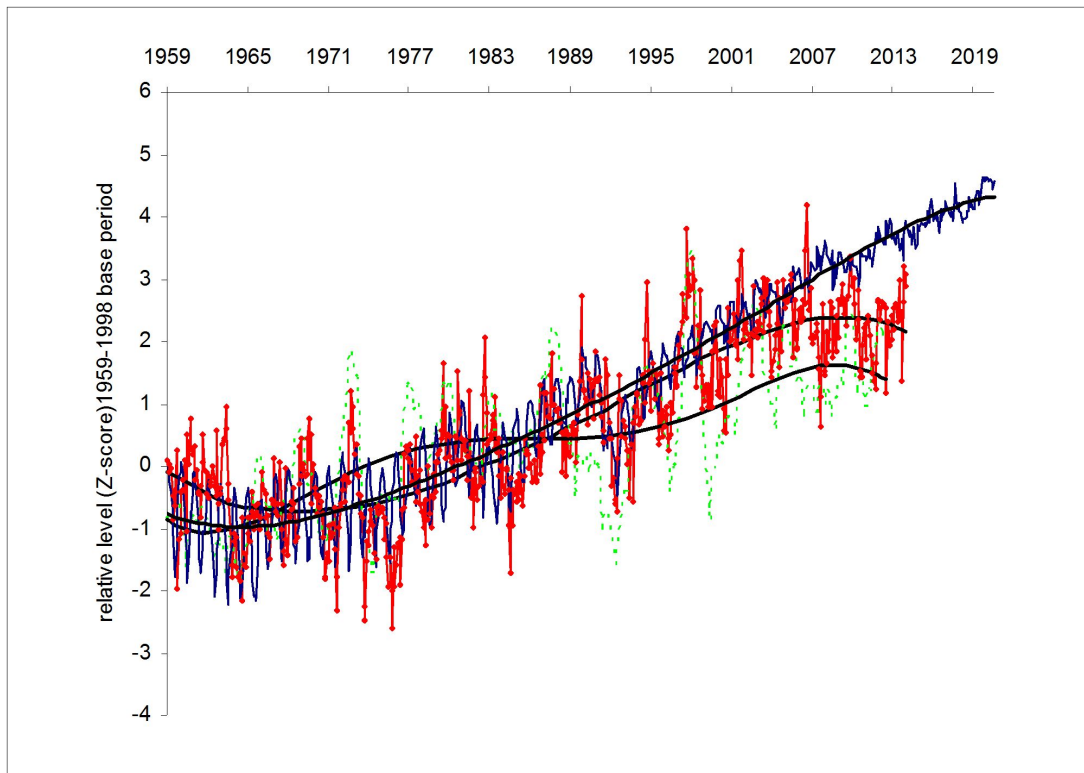
**Figure 1.** Monthly data: global surface temperature (HadCRUT4 dataset) (red dotted curve) and an IPCC mid-range scenario model (CMIP3, SRESA1B scenario) run for the IPCC fourth assessment report (IPCC 2007) (blue curve), each expressed in terms of Z scores to aid visual comparison (see Sect. 1).



10  
11  
12  
13  
14  
15  
16  
17  
18  
19  
20  
21  
22  
23  
24  
25  
26  
27  
28  
29  
30

1  
2  
3  
4  
5  
6  
7  
8  
9  
10  
11  
12  
13

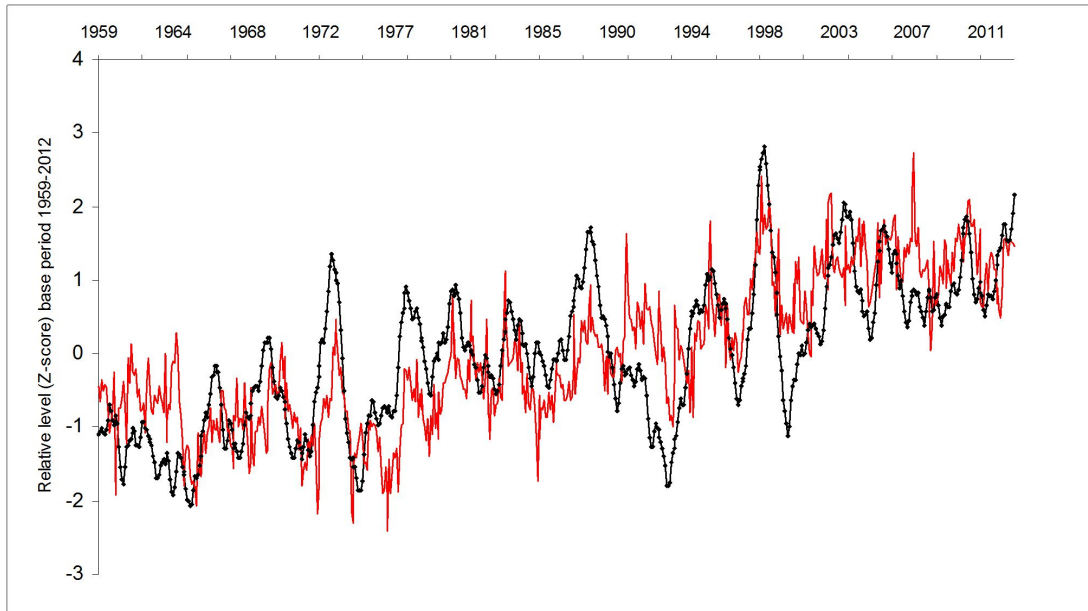
**Figure 2.** Z scored monthly data: global surface temperature (green dashed curve) compared to an IPCC mid-range scenario global climate model (GCM) – the CMIP3, SRESA1B scenario run for the IPCC fourth assessment report (IPCC 2007) (blue curve) and also showing the trend in first-difference atmospheric CO<sub>2</sub> (smoothed by two 13 month moving averages) (red dotted curve). To show their core trends for illustrative purposes the three series are fitted with 5th order polynomials.



14  
15  
16  
17  
18  
19  
20  
21  
22  
23  
24  
25  
26  
27  
28  
29  
30

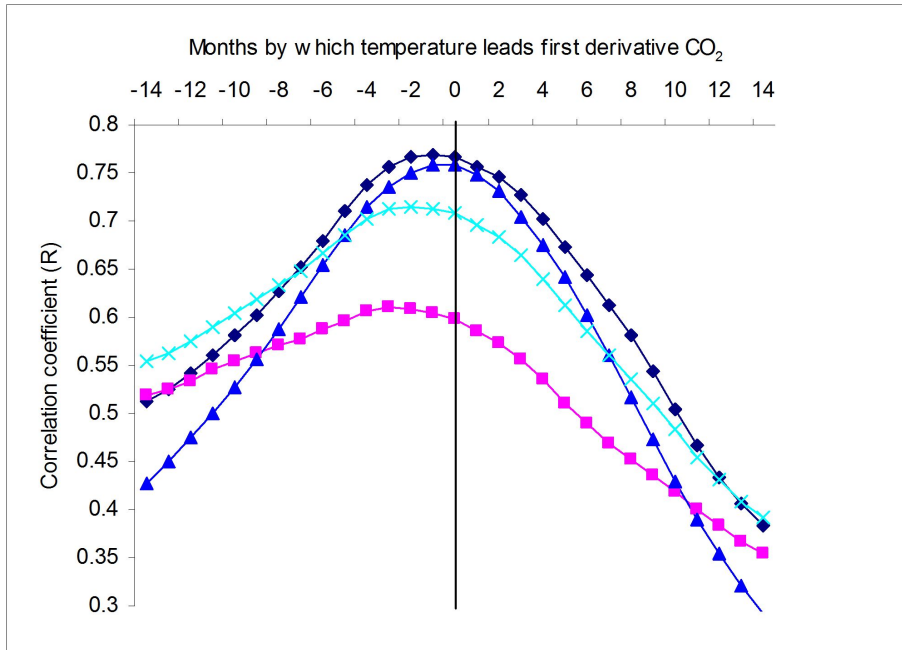
1  
2  
3  
4  
5  
6  
7  
8

**Figure 3.** Z scored monthly data: global surface temperature (red curve) compared to first-difference atmospheric CO<sub>2</sub> smoothed by two 13 month moving averages (black dotted curve).



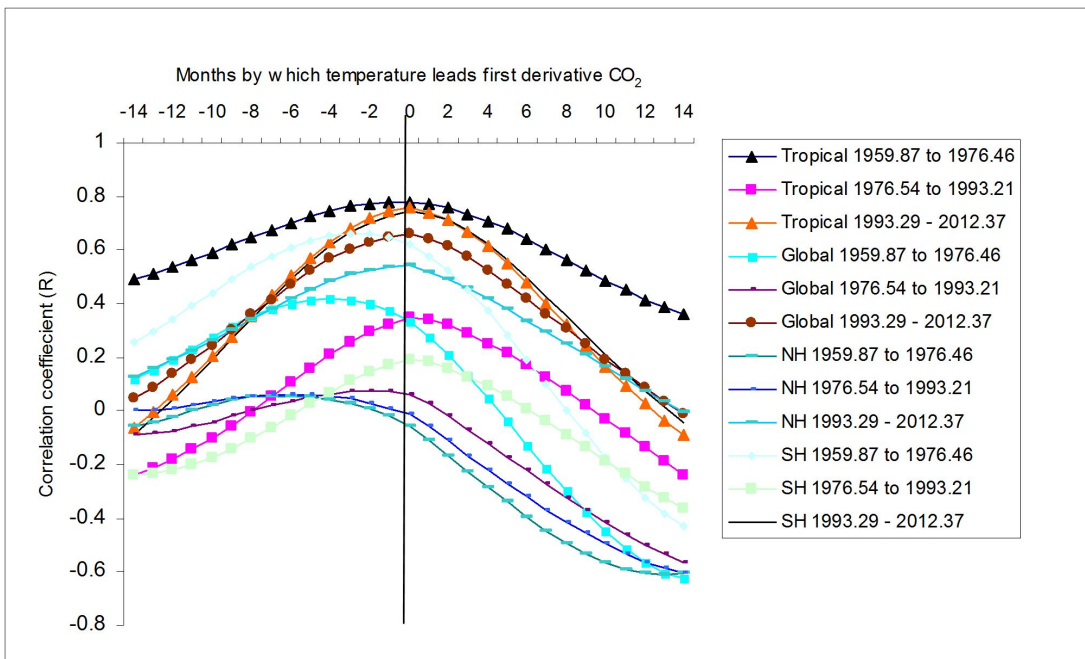
9  
10  
11  
12  
13  
14  
15  
16  
17  
18

**Figure 4.** Correlograms of first-difference CO<sub>2</sub> with surface temperature for global (turquoise curve with crosses), tropical (blue curve with triangles), Northern Hemisphere (purple curve with boxes) and Southern Hemisphere (black curve with diamonds) categories



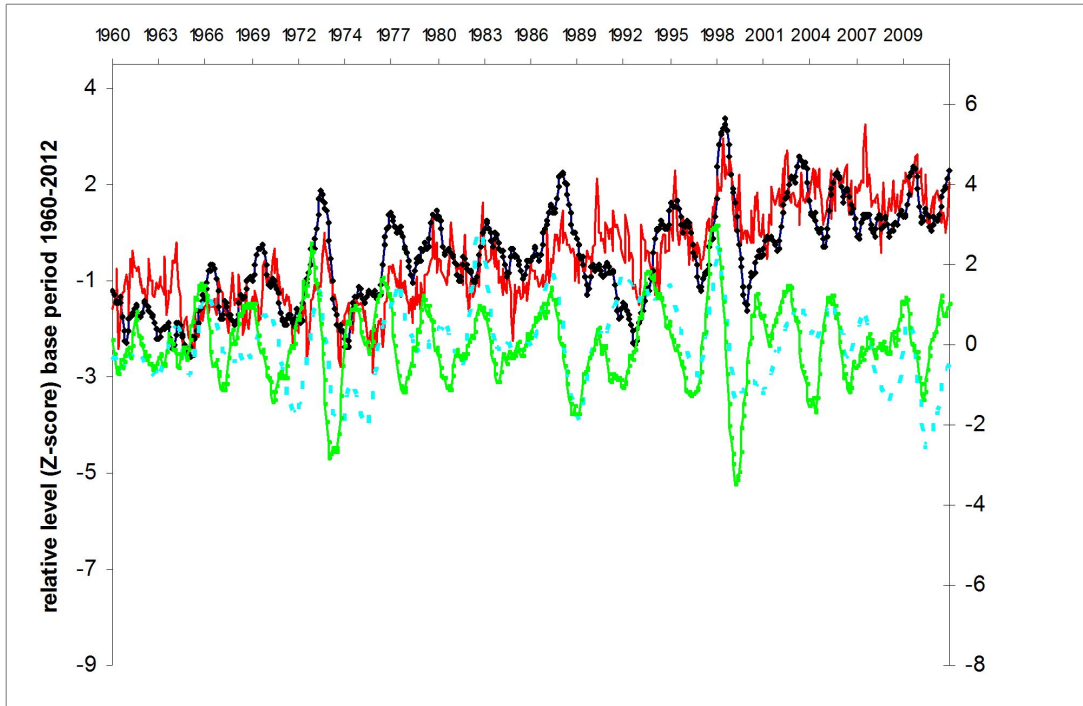
1  
2  
3  
4  
5  
6  
7

**Figure 5.** Correlograms of first-difference CO<sub>2</sub> with surface temperature for global, tropical, Northern Hemisphere and Southern Hemisphere categories, each for three time-series sub-periods.



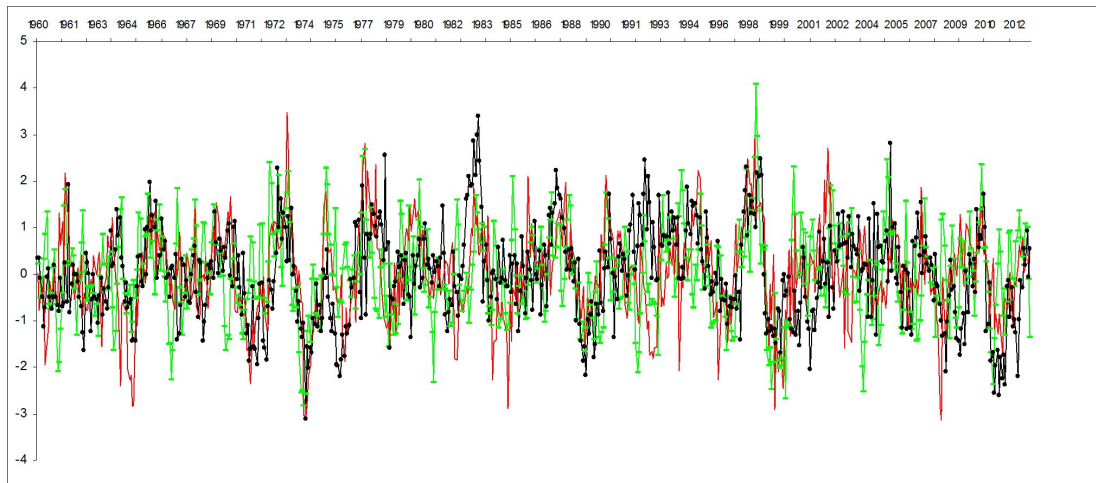
8  
9  
10  
11  
12  
13  
14

**Figure 6.** Z scored monthly data: global surface temperature (red curve) and first-difference atmospheric CO<sub>2</sub> smoothed by two 13 month moving averages (black dotted curve) (left-hand scale); sign-reversed SOI smoothed by a 13 month moving average (blue dashed curve) and second-difference atmospheric CO<sub>2</sub> smoothed by three 13 month moving averages (green barred curve) (right-hand scale)



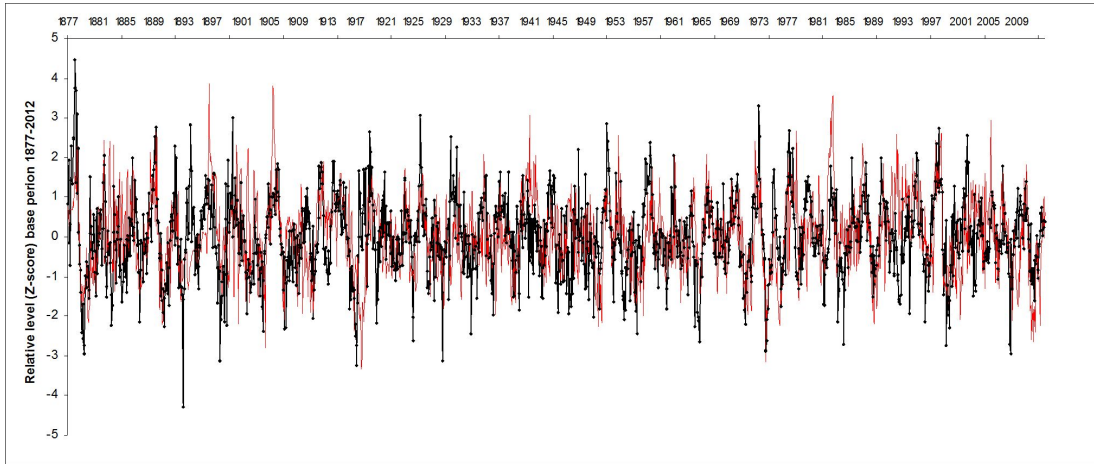
1  
2  
3  
4  
5  
6  
7  
8  
9

**Figure 7.** Z scored monthly data from 1960 to 2012: sign-reversed SOI (unsmoothed and neither led nor lagged) (dotted black curve); second-difference CO<sub>2</sub> smoothed by a 13 month × 13 month moving average and led relative to SOI by 2 months (green dashed curve ); and first-difference global surface temperature smoothed by a 13 month moving average and led by 3 months (red curve).



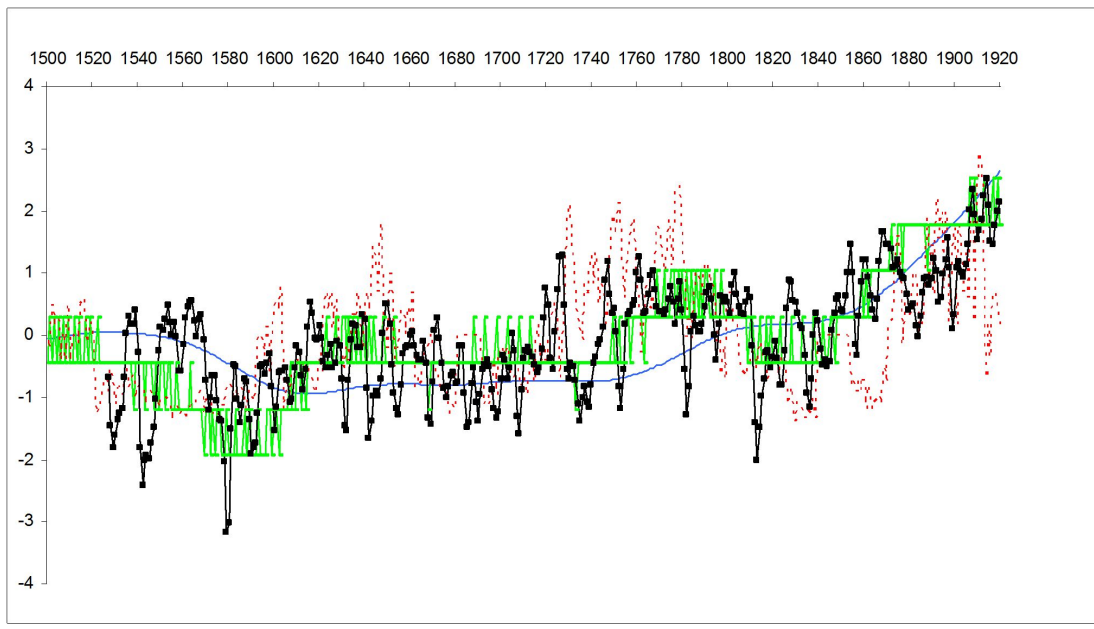
10  
11  
12  
13  
14  
15  
16  
17  
18  
19

**Figure 8.** Z scored monthly data from 1877 to 2012: sign-reversed SOI (unsmoothed and neither led nor lagged) (red curve); and first-difference global surface temperature smoothed by a 13 month moving average and led relative to SOI by 3 months (black dotted curve)



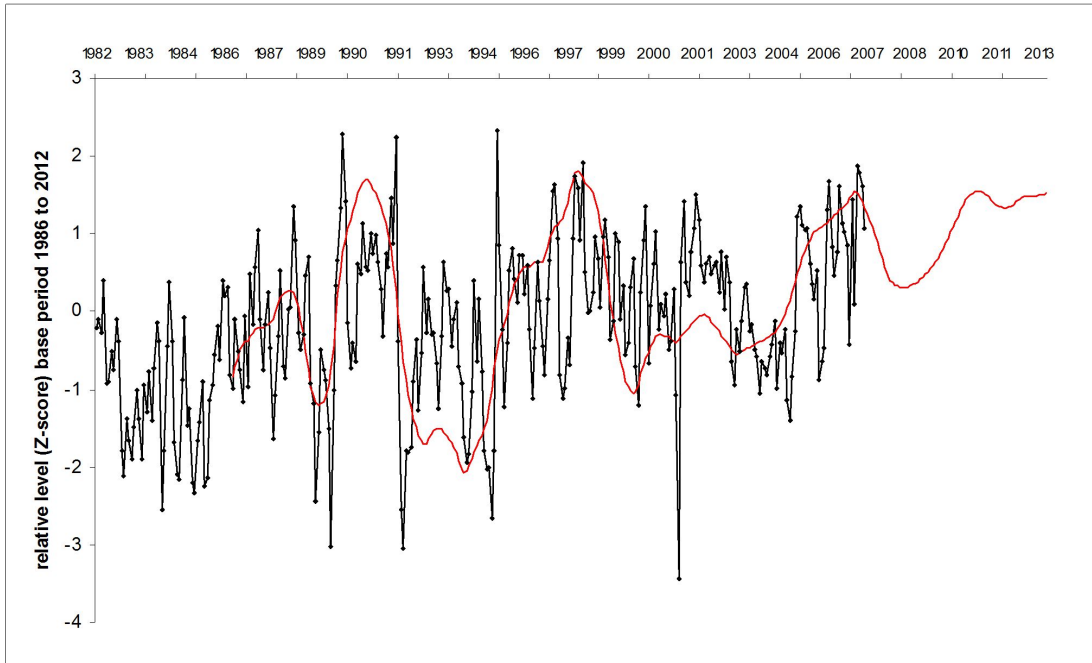
1  
2  
3  
4  
5  
6  
7  
8  
9  
10  
11  
12  
13  
14  
15

**Figure 9.** Z scored annual data: paleoclimate time series from 1500: ice core level of CO<sub>2</sub> (blue curve), level of CO<sub>2</sub> transformed into first-difference form (green barred curve); and temperature from speliotem (red dashed curve) and tree ring data (black boxed curve).

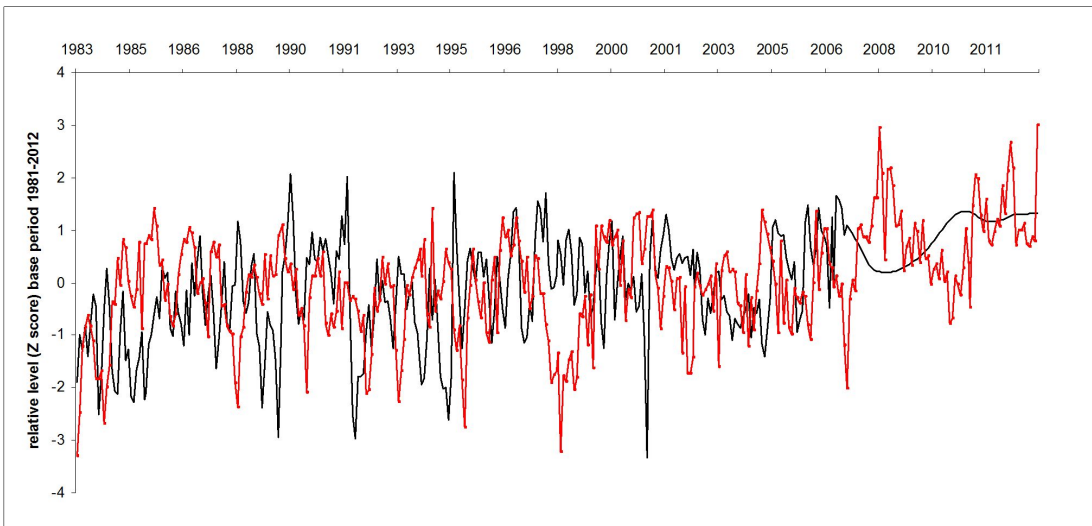


16  
17  
18  
19  
20  
21

1 **Figure 10:** Z scored monthly data: NDVIG (black dotted curve) compared to NDVIV  
2 (red curve).  
3

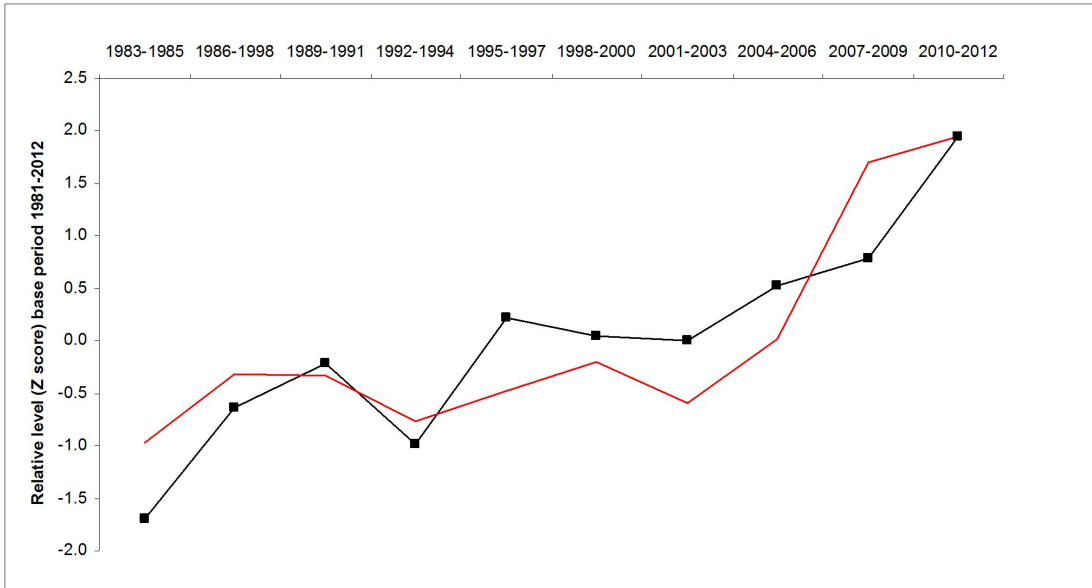


4  
5  
6 **Figure 13.** Z scored monthly data: NDVI (black curve) compared to the difference  
7 between the temperature projected from an IPCC mid-range scenario model (CMIP3,  
8 SRESA1B scenario) run for the IPCC fourth assessment report (IPCC 2007) and  
9 global surface temperature (red dotted curve).  
10



11  
12  
13  
14  
15  
16 **Figure 14.** Z scored data for periods each of 36 months, averaged: NDVI (black  
17 curve) compared to the difference between the temperature projected from an IPCC  
18 mid-range scenario model (CMIP3, SRESA1B scenario) run for the IPCC fourth  
19 assessment report (IPCC 2007) and global surface temperature (red dotted curve).

1



2

3

4

5

6

7

8

9

10

11

12

13

14

15

16

17

18

19

20

21

22

23

24

25

26

1

2

3